

# Fuelling with iron

An *in-vitro* study to examine the influence of iron supplementation on *Escherichia coli* using Fe-55 as a tracer

I.D. Thakoer



# Fuelling with iron

An *in-vitro* study to examine the influence of iron supplementation on *Escherichia coli* using Fe-55 as a tracer

By

Indira Devi Thakoer

4752716

in partial fulfilment of the requirements for the degree of

**Master of Science**

in Chemical Engineering

at the Delft University of Technology,

to be defended publicly on Thursday, August 25, 2022, at 2:30 PM

Supervisor:	Dr. ir. R. de Kruijff	
Thesis committee:	Dr. ir. R. de Kruijff,	TU Delft
	Dr. P. Hagendoorn	TU Delft
	Dr. K. Djanashvili	TU Delft



## **Abstract**

Iron deficiency is considered the most significant nutritional deficiency worldwide, affecting billions of people. Iron deficiency leads to a higher prevalence of iron deficiency anaemia; a condition responsible for over 50,000 deaths annually. Since anaemia is considered a global health problem, various countermeasures have been implemented to battle this disease. One of these countermeasures is the supplementation of iron. Different iron compounds are employed for supplementation, including ferrous sulphate and ferrous fumarate. However, since only 15% of the supplemented iron is absorbed by the human body, the remaining 85% can cause various health-related issues. Due to heightened amounts of iron present in the duodenum, a disbalance in the human gut is induced, leading to e.g. excessive growth of *E.coli*.

This study investigates the influence of 3 and 30  $\mu\text{M}$  iron supplementation of ferric chloride and ferric sulphate; radiolabelled with  $^{55}\text{Fe}$ . These results have been reported in the form of growth curves, and the remaining amount of  $^{55}\text{Fe}$  in the growth medium has been used to estimate iron uptake by *E.coli*. No significant differences were observed between 3 and 30  $\mu\text{M}$  iron supplementation of both compounds, indicating that iron concentration may not be considered as the main limiting growth factor of *E.coli*. Therefore, further research is recommended where the medium is analysed for the presence of other nutrients. Additionally, adjustments in the growth environment are recommended, to determine which growth conditions influence *E.coli* the most.



# Table of Contents

<b>Abbreviations and acronyms</b> .....	8
<b>1. Introduction</b> .....	9
<b>2. Theoretical Framework</b> .....	10
2.1. <i>The role of iron in the human body</i> .....	10
2.1.1. <i>Iron and oxidative stress</i> .....	10
2.1.2. <i>Bioavailability of iron</i> .....	11
2.1.3. <i>Iron requirements</i> .....	11
2.2. <i>Iron deficiency and iron deficiency anaemia</i> .....	12
2.3. <i>Iron supplementation</i> .....	13
2.3.1. <i>Oral iron supplementation</i> .....	13
2.3.2. <i>Intravenous iron supplementation</i> .....	14
2.3.3. <i>Reducing the side effects of iron supplementation</i> .....	14
2.4. <i>Gastrointestinal tract</i> .....	15
2.4.1. <i>The intestinal flora in the gastrointestinal tract</i> .....	15
2.5. <i>Iron as an isotopic tracer</i> .....	18
2.6. <i>Methods for analysis</i> .....	18
2.6.1. <i>X-ray diffraction</i> .....	18
2.6.2. <i>Liquid Scintillation Counting</i> .....	19
2.6.3. <i>Inductively Coupled Plasma-Optical Emission Spectrometry</i> .....	20
<b>3. Materials &amp; Methods</b> .....	22
3.1. <i>Materials</i> .....	22
3.2. <i>Methods</i> .....	23
3.2.1. <i>Synthesis of ferrous and ferric iron compounds</i> .....	23
3.2.2. <i>Analysis</i> .....	25
3.2.3. <i>Preparation of iron supplementation solutions</i> .....	25
3.2.4. <i>Culturing of Escherichia coli</i> .....	26
3.2.5. <i>Liquid Scintillation Counting as a method of analysis</i> .....	28
<b>4. Results and discussion</b> .....	30
4.1. <i>Synthesis of ferrous and ferric compounds</i> .....	30
4.1.2. <i>Synthesis of ferrous sulphate</i> .....	31
4.1.3. <i>The synthesis of ferrous fumarate</i> .....	31
4.2. <i>Growth curve experiments of Escherichia coli</i> .....	32
4.2.2. <i>Construction of the growth curves</i> .....	33
4.3. <i>Liquid Scintillation Counting</i> .....	38
4.3.1. <i>The uptake of supplemented <sup>55</sup>Fe</i> .....	38

4.4. <i>Further implications</i> .....	40
<b>5. Conclusions and Recommendations</b> .....	<b>41</b>
5.1. <i>Conclusions</i> .....	41
5.2. <i>Recommendations</i> .....	41
<b>Bibliography</b> .....	<b>43</b>
<b>Appendix A – Growth curve experiments with non-radioactive iron supplementation</b> .....	<b>49</b>
<b>Appendix B – Growth curve experiments with radionuclide iron supplementation</b> .....	<b>51</b>
<b>Appendix C – Liquid Scintillation Counting – Construction of a quench correction curve</b> .....	<b>53</b>

## Abbreviations and acronyms

DNA	Deoxyribonucleic acid
EC	Electron Capture
<i>E.coli</i>	<i>Escherichia coli</i>
ICDD	International Centre for Diffraction Data
ICP-OES	Inductively Coupled Plasma-Optical Emission Spectrometry
ID	Iron deficiency
IDA	Iron deficient anaemia
IPC	Iron polymaltose complex
IV	Intravenous
LB	Luria-Bertani
LSC	Liquid Scintillation Counting
$\mu$	Specific growth rate
$\mu_{\max}$	Maximum specific growth rate
OD	Optical density
OLS	Ordinary Least-Squares
ROS	Reactive Oxygen Species
SD	Standard Deviation
SI	Sucrosomial ® Iron
SSR	Sum of squared residuals
$t_i$	Inflection time
XRD	X-ray Diffraction
WHO	World Health Organization

## 1. Introduction

Anaemia is considered a global public health problem by the World Health Organization (WHO), by which globally approximately 47% of preschool children and over 40% of pregnant women in particular are affected (*Anaemia*, n.d.; Brannon & Taylor, 2017). Anaemia is a condition characterised by either a significantly lowered amount of red blood cells, or a decreased level of haemoglobin (*Anaemia*, n.d.). Even though various causes can be attributed to anaemia, the WHO has estimated that approximately 50% of the beforementioned cases of anaemia are caused by iron deficiency (ID), which will be referred to as iron deficient anaemia (IDA). When an individual suffers from IDA, the iron stores can be considered as being fully depleted, resulting in an inadequate supply to tissues since an insufficient amount of red blood cells is present (Brannon & Taylor, 2017; Stoltzfus, 2003). As a result, oxygen transportation is impaired (R.J. Stoltzfus & Dreyfuss, 1998). Various implications of IDA are child, maternal, and perinatal mortality, reduced fitness and productivity, and cognitive impairment (Rebecca J Stoltzfus, 2003).

To battle anaemia, various strategies can be employed, including iron supplementation (Abbaspour et al., 2014). Iron can either be supplemented orally or intravenously. The most common method is the supplementation of oral iron salts since it is considered to be effective and safe. In addition, the costs of oral iron supplementation are relatively low. However, only an approximate of 15% iron is absorbed in the duodenum, leaving a major part of the supplemented iron unabsorbed (Yilmaz & Li, 2018). However, despite oral iron supplementation being advantageous for replenishing iron stores, an excess of iron is associated with side effects related to the gastrointestinal tract (Busti et al., 2019).

The influence of unabsorbed iron on the gastrointestinal tract has been a subject of a variety of studies (Finlayson-Trick et al., 2020; Jaeggi et al., 2015; Tolkien et al., 2015). Accordingly, iron-dependent pathogens, such as the Enterobacteriaceae family, could benefit from the excess amount of iron, resulting in a disbalance in the human gut (Finlayson-Trick et al., 2020). This could result in serious implications for the human gastrointestinal tract, and could lead to side effects such as diarrhoea (Finlayson-Trick et al., 2020; Tolkien et al., 2015).

This thesis aimed to conduct an *in vitro* study making usage of *Escherichia coli* (*E.coli*) and radioactive  $^{55}\text{Fe}$  in order to mimic iron supplementation. Both the growth of *E.coli* has been investigated, as well as the uptake of supplemented  $^{55}\text{Fe}$ . This thesis contains a theoretical framework required to provide the reader with relevant background information for total comprehension of the paper. This chapter is followed by the methods and materials section, where experimental procedures are described for synthesising ferric and ferrous compounds, and for *E.coli* growth experiments. Afterwards, the obtained results of the experiments are shown and discussed. Finally, this thesis is concluded with conclusions that can be drawn from the results and proposed recommendations for further research.

## 2. Theoretical Framework

### 2.1. The role of iron in the human body

In the human body, iron mainly forms complexes bound to either 1) protein (haemoprotein) as one of the heme compounds haemoglobin or myoglobin, 2) heme enzymes, and 3) nonheme compounds such as flavin-iron enzymes, transferrin, and ferritin (Abbaspour et al., 2014).

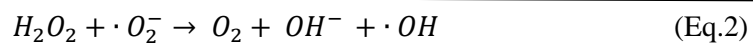
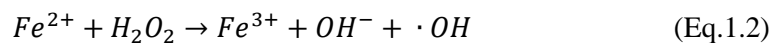
A variety of characteristic functions can be ascribed to the haemoprotein type of complex, Haemoglobins and myoglobins are mainly responsible for oxygen binding and transport, and influence oxygen metabolism, electron transport, and mitochondrial respiration (Yiannikourides & Latunde-Dada, 2019). Heme enzymes include catalase and peroxidase enzymes, which are involved in oxygen metabolism (Yiannikourides & Latunde-Dada, 2019).

When considering nonheme compounds, proteins containing nonheme iron also fulfil important functions, since they participate in DNA synthesis, gene regulation, drug metabolism, and cell proliferation and differentiation (Yiannikourides & Latunde-Dada, 2019).

However, there is a problem encountered when regarding iron in the human body. Iron has the ability to catalyse toxic oxidation reactions (Tapiero et al., 2001). This interferes with deoxyribonucleic acid (DNA), and can therefore induce damage to the human body; which is elaborated upon in the following section (Krumova & Cosa, 2016).

#### 2.1.1. Iron and oxidative stress

Iron has the capability to both accept and donate electrons, and can therefore primarily be found in two oxidation states in the human body: divalent ferrous iron ( $Fe^{2+}$ ), and trivalent ferric iron ( $Fe^{3+}$ ) (Bloor et al., 2021a; Vogt et al., 2021). As a result, iron has the ability to act as a catalyst in the Haber-Weiss cycle, which comprises of two reactions as depicted in Eq.1.1 and Eq.1.2, yielding the net reaction depicted in Eq.2. The Fenton reaction (Eq.1.2) describes the reaction between  $Fe^{2+}$  and hydrogen peroxide ( $H_2O_2$ ), where hydroxide ( $OH^-$ ) and hydroxyl radical ( $\cdot OH$ ) are formed (Gupta et al., 2016).



The hydroxyl radical ( $\cdot OH$ ) formed in the Fenton reaction, is considered to be one of the Reactive Oxygen Species (ROS), which are species that are considered to have toxic effects in aerobic organisms, including humans (Krumova & Cosa, 2016). The formation of free radical species is paired with serious consequences concerning human health due to the disruption of cellular structures (Papanikolaou & Pantopoulos, 2005). Since the guanine base present in DNA is prone to oxidation, free radical species can induce DNA damage in the form of base modifications and strand cleavage

(Kehrer, 2000; Meneghini, 1997). In addition, lipids and proteins are also sensitive to oxidation, and can therefore be negatively affected by free radical species as well (Kehrer, 2000).

### *2.1.2. Bioavailability of iron*

Iron compounds vary significantly in bioavailability. Stoffel et al. (2020) define the bioavailability of an iron compound as “the proportion of iron present in an oral supplement that is absorbed and incorporated into erythrocytes” (Stoffel et al., 2020, p. 1). As described by Hurrell & Egli (2010), dietary iron is present as nonheme iron, or as heme iron. However, nonheme iron accounts for approximately 90% of all dietary iron (Kortman et al., 2014).

Various distinctions can be made between heme – and nonheme iron. Whereas nonheme iron is mainly found in plant-based sources and animal tissues, heme iron is found in animal-based sources in the form of haemoglobin and myoglobin (Hurrell & Egli, 2010). In addition, heme iron has a bioavailability reported of 15%-35%, whereas the absorption of nonheme iron is lower and lies in the range of 2%-20% (Abbaspour et al., 2014).

The absorption of nonheme iron is dependent on other components. Hurrell & Egli (2010) list phytate, polyphenols, calcium and proteins as iron absorption inhibitors. Ascorbic acid (vitamin C) and muscle tissue are listed as enhancers, since both have the ability to reduce ferric ( $\text{Fe}^{3+}$ ) iron to ferrous ( $\text{Fe}^{2+}$ ) iron, enabling the formation of soluble ferrous complexes which are more suitable for absorption (Abbaspour et al., 2014; Santiago, 2012). For an in-depth overview of the specific influence of both inhibitors and enhancers, further reading is recommended (Abbaspour et al., 2014; Tapiero et al., 2001).

### *2.1.3. Iron requirements*

The metabolism of iron in the human body differs significantly from the metabolism of other metals in the human body. Firstly, there is no physiological mechanism for iron excretion (Hurrell & Egli, 2010). Secondly, since approximately 90% of daily iron requirements are obtained from the breakdown of red blood cells circulating in the human body, the remainder (1-2 mg/day) has to be obtained from dietary iron absorbed in the duodenum (Dev & Babitt, 2017; Hurrell & Egli, 2010; Vogt et al., 2021). Vogt et al. (2021) report iron quantities of over 1 billion iron atoms per red blood cell. An approximate of 1-2 mg of iron is lost daily through epithelial desquamation and blood loss (Dev & Babitt, 2017). These losses should be compensated for with dietary iron to maintain proper iron homeostasis (Abbaspour et al., 2014; Hurrell & Egli, 2010).

As mentioned earlier, no defined mechanism is present for iron excretion. Therefore, iron homeostasis is mainly regulated through absorption, where hepcidin can be considered the primary regulator (Stoffel et al., 2020). When an increase in the amount of iron, e.g. due to supplementation, is observed in the human body, the production of hepcidin is induced. As a result of increased hepcidin production, iron absorption is blocked (Pagani et al., 2019) However, when the amount of iron present in the human body is lowered, the production of hepcidin is suppressed and iron is released from iron

stores in the human body (Camaschella, 2015). For a more in-depth overview of iron metabolism, further reading is recommended (Abbaspour et al., 2014; Tapiero et al., 2001).

Throughout an individual's life, the iron requirements change. In Table 1, the average iron requirements of various groups are listed (Abbaspour et al., 2014). The iron requirements are reported in terms of the amount that should be absorbed in the gastrointestinal tract; therefore, already accounting for bioavailability. With regards to infants and adolescents, the relatively high iron requirements can be ascribed to the need for iron during rapid growth. Considering pregnancy, iron is also needed for the growth of the placenta and unborn child, resulting in a significant increase in iron demand (Abbaspour et al., 2014). Therefore, considering these groups, when one's diet does not contain an adequate amount of (absorbable) iron, one can quickly suffer from ID or IDA (Abbaspour et al., 2014).

**Table 1.** Iron requirements of 97.5% of individuals in terms of absorbed iron, by age group and sex. The table was adapted from Abbaspour et al. (2014, p. 168).

Age/sex	mg/day
4-12 months	0.96
13-24 months	0.61
2-5 years	0.70
6-11 years	1.17
12-16 years (girls)	2.02
12-16 years (boys)	1.82
Adult males	1.14
First trimester of pregnancy	0.80
Second and third trimester of pregnancy	6.30
Lactating women	1.31
Menstruating women	2.38
Postmenopausal women	0.96

## 2.2. Iron deficiency and iron deficiency anaemia

When one is systematically not able to meet one's iron requirements, serious consequences are expected. As mentioned earlier, hepcidin is responsible for the regulation of iron homeostasis. When an individual is suffering from ID, the transcription of hepcidin is suppressed. As a result, iron is released from iron stores in the human body. Therefore, the speed at which stores are depleted indicates the speed at which ID is developed (Camaschella, 2015). ID causes various symptoms, such as lower cognitive development in young children, and overall ill health (Camaschella, 2015).

When ID is left untreated, the chances of developing IDA become higher. In the case of IDA, the iron stores are severely depleted, leading to the inability of the human body to produce haemoglobin; causing poorer delivery of oxygen to body tissues (*Anaemia*, n.d.; Camaschella, 2015).

The consequences that are reported for IDA are severe. IDA impacts cognitive development negatively, and leads to poor pregnancy outcomes, impaired immunity, and reduced work capacity in

adults (Stelle et al., 2018). Furthermore, next to these severe consequences, morbidity levels are heightened as well. It is reported that IDA is worldwide responsible for 50,000 deaths annually, while ID annually contributes to 120,000 female deaths related to pregnancy (Stelle et al., 2018). Therefore, it can be concluded that the treatment of ID and IDA should be prioritised.

### *2.3. Iron supplementation*

To prevent and treat ID and IDA, iron supplementation is used as a strategy (Bashiri et al., 2003). Both oral and intravenous (IV) supplementation are possible. However, the standard treatment is oral iron supplementation (Berber et al., 2014; Santiago, 2012). Oral iron supplementation is noted to be easy to use, have relatively fewer adverse health effects, and have high effectiveness (Berber et al., 2014). Research has been conducted into the differences between oral and IV supplementation, which will be elaborated upon in the following sections.

#### *2.3.1. Oral iron supplementation*

##### *2.3.1.1. Bivalent vs. trivalent oral iron preparations*

For supplementation, the preference is given to ferrous iron salts instead of ferric iron salts, since only the divalent form ( $\text{Fe}^{2+}$ ) is suitable for uptake by intestinal enterocytes (Santiago, 2012). For ferric iron to be absorbed, it should first be reduced to ferrous iron; therefore, adding a conversion step in the absorption of iron in the human body. In addition, in comparison to ferrous salts, the solubility of ferric iron is relatively poorer in alkaline media, leading to a 3 to 4 times lower bioavailability (Nagpal & Choudhury, 2004; Santiago, 2012). In practice, for the treatment of IDA administration of 100 mg/day of ferrous iron would be sufficient, while for ferric iron a dose of 400-1000 mg/day should be considered (Nagpal & Choudhury, 2004). The most frequently used iron supplement forms are ferrous sulphate, ferrous fumarate, and ferrous gluconate (Camaschella, 2015; Zariwala et al., 2013). Santiago (2012) notes that ferric iron supplements with an iron polymaltose complex (IPC) are also frequently used.

However, besides the importance of iron preparations providing adequate bioavailability, gastrointestinal tolerance should also be taken into account. Finlayson-Trick et al. (2020) report that the relatively inexpensive ferrous sulphate ( $\text{FeSO}_4$ ) causes a variety of gastrointestinal side effects, such as diarrhoea, inevitably making supplementation more difficult. In contrast, fewer side effects are reported for supplementation with ferrous fumarate which is considered to be more readily absorbed (Patil et al., 2013).

In addition, with regards to oral iron supplementation, characteristics such as taste and odour should be taken into account. Nagpal & Choudhury (2004) report that ferrous sulphate has a salty taste, whereas ferrous fumarate is practically tasteless.

##### *2.3.1.2. Adverse effects of oral iron supplementation*

Despite oral supplementation being the most common method for treatment (section 2.3.),

approximately 10–40% of the patients suffer from adverse effects primarily related to the gastrointestinal tract (Bashiri et al., 2003). In order to minimize these adverse side effects, certain medications can be taken. However, this medication negatively influences the absorption of the supplemented iron, resulting in a lessened effect of the treatment. The most common reported side effects are nausea, constipation, and epigastric pain (Bloor et al., 2021a; Finlayson-Trick et al., 2020; Stoffel et al., 2020). These side effects can primarily be ascribed to the influence of unabsorbed dietary iron, modifying the gut microbiota equilibrium (Yilmaz & Li, 2018), as further explained in section 2.4.1.

### *2.3.2. Intravenous iron supplementation*

IV iron supplementation is considered more suitable for individuals suffering from intolerance to oral iron, malabsorption in the gastrointestinal tract, and severe anaemia where rapid repletion of the iron stores is required (Estadella et al., 2018; Schaefer et al., 2020).

Since IV iron supplementation is administered directly into the bloodstream, gastrointestinal side effects can be reduced by bypassing the gastrointestinal lumen (Bloor et al., 2021b). This results in a quicker increase in haemoglobin levels in comparison with oral iron supplementation (Camaschella, 2015). As a result, possible complications during anaemia treatment can be reduced through IV iron supplementation (Estadella et al., 2018).

In order to achieve effective, non-toxic, delivery of IV supplemented iron, iron is incorporated in composite nanoparticles, composed of ferric oxy-hydroxides and carbohydrates (Jahn et al., 2011; Neiser et al., 2015; Schaefer et al., 2020). The usage of composite nanoparticles is necessary since in circulation iron is strongly bound to the transport protein transferrin (Schaefer et al., 2020).

#### *2.3.2.1. Adverse effects of intravenous iron supplementation*

Despite the various advantages that are provided by IV supplementation, there are reports regarding certain side effects that can not be overlooked. Some of the side effects are nausea, vomiting, and back and chest pain. However, the longevity of these effects is significantly lower and is reported to last a maximum of 48 hours after completion of the medication (Camaschella, 2015).

#### *2.3.3. Reducing the side effects of iron supplementation*

Although the aim is to design iron supplementation with limited consequences regarding overall health, it is also possible to target the consequences afterwards.

Firstly, the presence of excessive free radicals (section 2.1.1.), can be targeted by hindering the formation of free radicals with antioxidants (Qi et al., 2020). In addition, research has shown that usage of substances that release iron more slowly causes the formation of free radicals to slow down. One substance that meets the latter requirement, is Sucrosomial® Iron (SI). Gómez-Ramírez et al. (2018) report that in this substance, iron is comprised in a ferric pyrophosphate complex, which is protected by a phospholipid bilayer membrane. Consequently, as a gastro-resistant complex, and by

avoiding general iron absorption pathways, higher tolerability is reported in comparison to traditional iron supplements (Gómez-Ramírez et al., 2018; Qi et al., 2020).

Secondly, aiming to restore the balance between probiotics and pathogens in the gastrointestinal tract is also considered a possibility. Although various methods are elaborated upon in literature, the most straightforward solution would be the administration of either prebiotics or probiotics (Helmyati et al., 2018; Jia et al., 2016; Martínez-Navarrete et al., 2002; Pérez-Conesa et al., 2006). The latter is known to be improving microbial composition, whereas the first are selective non-fermented food ingredients that primarily serve as food for probiotics (Rusu et al., 2020). Qi et al. (2020) report lowering of the pH in the colon, the formation of a biological barrier, and the inhibition of pathogens as the most beneficial consequences.

#### 2.4. Gastrointestinal tract

The circumstances of the gastrointestinal tract vary throughout the human body. In Table 2, the pH of various parts of the colonic lumen is shown. In the presence of oxygen, ferrous iron oxidates quickly to ferric iron at neutral pH, whereas under acidic conditions ferrous iron is stable and does not oxidize (Straub et al., 2000)

After ingestion of dietary iron, firstly the stomach is reached. The environment of the stomach can be considered acidic and oxygenic, providing optimal circumstances for iron to reach the intestine in the ferrous form. Throughout the gastrointestinal tract, the pH rises, which leads to both a decrease in the solubility of ferric iron and a more rapid oxidation of iron (Yilmaz & Li, 2018). However, it should be taken into account that besides the pH and the amount of oxygen, the solubility and availability of iron are dependent on a combination of a variety of factors. As described in section 2.1.2, dietary factors can either inhibit or enhance iron absorption.

**Table 2.** The pH along the gastrointestinal tract. Information has been adapted from Yilmaz & Li (2018).

Part of the colonic lumen	pH
Stomach	1.5 – 3.5
Duodenum	1.5 – 4.5
Small intestine	6.2 – 7.5
Colon	4.5 – 7.5

##### 2.4.1. The intestinal flora in the gastrointestinal tract

The intestinal flora consists of a great variety of probiotics and pathogens. The balance between probiotics and pathogens is of importance for human health since probiotics have beneficial functions such as enhancing the synthesis of vitamins, promoting gastrointestinal mobility, and preventing an invasion of pathogens, whereas pathogens are mainly responsible to disturb this balance leading to e.g. constipation and diarrhoea (Qi et al., 2020).

The majority of pathogenic enterobacteria, such as *E.coli* and *Salmonella*, rely on the

acquisition of iron in order to colonize one's gastrointestinal tract (Jaeggi et al., 2015; Paganini & Zimmerman, 2017). Therefore, iron can be considered essential for the replication of a variety of gut bacteria (Jaeggi et al., 2015; Yilmaz & Li, 2018). In comparison to the beforementioned bacteria, probiotic, non-pathogenic *Lactobacilli* and *Bifidobacteria* – which are regarded as beneficial bacteria for the human gut – require manganese instead of iron for their growth and colonization (Jaeggi et al., 2015; Paganini & Zimmerman, 2017). As a result, an increased amount of unabsorbed iron could lead to a shift in the balance towards the growth of enterobacteria over probiotics, resulting in increased gut inflammation and other intestinal diseases (Paganini & Zimmerman, 2017; Qi et al., 2020). Therefore, the dosage of iron supplementation should be regulated and adjusted when necessary. Optimally, iron deficiencies should be resolved, while preventing a major impact on dominant probiotics, in order to assure optimal functionality of intestinal cells and prevent disorders of the intestinal barrier function (Qi et al., 2020).

#### 2.4.1.1. *Escherichia coli*

Considering various types of bacteria, distinctions can be made between either gram-positive and gram-negative bacteria; where *E.coli* belongs to the latter. A fundamental distinction can be made with regards to their cell walls: gram-negative bacterial cells contain an outer membrane, whereas gram-positive bacteria do not (Lugtenberg & van Alphen, 1983). Consequently, regarding gram-negative bacteria, a barrier is created between the inner part of the cell and its environment.

##### 2.4.1.1.1. *Siderophores*

In order to acquire iron, bacteria have developed a variety of strategies. When considering gram-negative bacteria, such as *E.coli*, the production of siderophores is considered to be the most effective and successful method of high-affinity iron acquisition (Miethke & Marahiel, 2007). Siderophores are small molecules (<1 kDa) functioning as high-affinity iron chelators (Miethke & Marahiel, 2007). Wandersman & Delepelaire (2004) report that the affinity constant is consistently higher than  $10^{30}$  M<sup>-1</sup>. The latter characteristic enables *E.coli* to compete in iron acquisition with certain proteins of the host, such as haemoglobin and transferrin (Chu et al., 2010). Martin et al. (2017) report a range for the association constant between  $10^{12}$  and  $10^{52}$ .

Siderophores form complexes with Fe<sup>3+</sup>, followed by active transportation of these iron-siderophore complexes into the cells (Miethke & Marahiel, 2007). The bound iron is then released through reduction to Fe<sup>2+</sup> (Braun, 2003). As a result, iron can effectively be solubilised and extracted from minerals or organic compounds (Wandersman & Delepelaire, 2004). For a more in-depth overview regarding the transport system of *E.coli* with regards to Fe<sup>2+</sup>, further reading is recommended (Braun, 2003).

Based on a siderophore's characteristic iron ligation group, four types can be distinguished: catecholate, phenolate, hydroxamate, and carboxylate (Miethke & Marahiel, 2007; Wandersman & Delepelaire, 2004). Which kind of siderophore is synthesised depends on the environmental

circumstances since each siderophore has a different affinity for  $\text{Fe}^{3+}$  (Martin et al., 2017). *E.coli* synthesises four types of siderophores: enterobactin, salmochelin, yersiniabactin and aerobactin (Demir & Kaleli, 2004; Martin et al., 2017).

The affinity of  $\text{Fe}^{3+}$  to siderophores can be explained by the characteristics both components possess.  $\text{Fe}^{3+}$  can be considered a strong Lewis acid, whereas the donor atoms of siderophores represent hard Lewis bases. As a result, the interactions between metal and ligand can be regarded as relatively strong. When a comparison is made between the preferred interactions of  $\text{Fe}^{2+}$  and  $\text{Fe}^{3+}$ , the former can be considered as not completely acidic. Consequently, the interaction between softer donor atoms is preferred, and the ability to form complexes with siderophores is relatively low (Miethke & Marahiel, 2007).

#### 2.4.1.1.2. Determining growth behaviour of *Escherichia coli*

Bacterial growth can be made insightful by constructing a growth curve. An example of a growth curve is depicted in Figure 1. The specific growth rate ( $\mu$ ) starts at zero, which throughout the lag time ( $\lambda$ ), proceeds to its maximum value ( $\mu_{\max}$ ). Finally,  $\mu$  decreases to zero again, resulting in an asymptote (A). Consequently, a model is constructed relating the logarithm of the number of organisms (N) to the time (Zwietering et al., 1990).

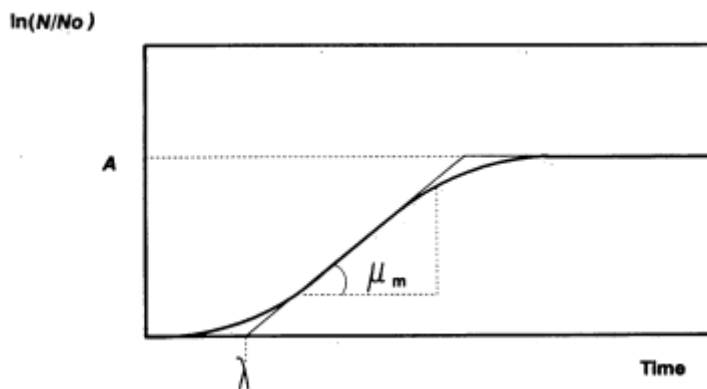


**Figure 1.** An example of a bacterial growth curve. The figure is adapted from Zwietering et al. (1990).

A model which is applicable to describe the behaviour of microorganisms is the logistic model (Eq.3), where  $\text{OD}_{600}$  (AU) is the measured optical density (OD) at 600 nm,  $\text{OD}_{600,\max}$  (AU) is the maximum OD at 600 nm,  $\mu_{\max}$  ( $\text{h}^{-1}$ ) is the maximum specific growth rate,  $t_l$  (h) is the inflection point of the curve, and  $t$  (h) is a certain timepoint (Dalgaard et al., 1994). This model provides the opportunity to describe the behaviour of microorganisms, such as *E.coli*, in relation to various circumstances, including iron supplementation.

$$\text{OD}_{600} = \frac{\text{OD}_{600,\max}}{(1 + e^{-\mu_{\max} \times (t - t_l)})} \quad (\text{Eq.3})$$

The logistic model enables making predictions considering the growth of *E.coli*, by estimating the three unknown growth parameters that are included in Eq.3. Firstly,  $OD_{600,max}$  (AU) gives an indication about the maximum biomass density that is achievable for *E.coli*. Secondly, the  $\mu_{max}$  ( $h^{-1}$ ) provides the highest growth rate that can be obtained. And lastly, the inflection time,  $t_i$  (h), indicates the point in time at which the increase of the  $\mu$  is finished, and starts decreasing.

#### 2.4.1.1.2.1. Application of the logistic model

Regression analysis can be applied to estimate values for the three growth parameters. One of the methods that can be used is Ordinary Least-Squares (OLS). OLS aims to reduce the sum of the squared residuals (SRR). Therefore, the difference between value of the measured data ( $y$ ) and the value obtained from the fit ( $y_i$ ) is as small as possible. This is visualised in Eq 4.

$$SSR = \sum_i (y - y_i)^2 \quad (\text{Eq.4})$$

### 2.5. Iron as an isotopic tracer

A method which can be employed to assess the uptake of iron by *E.coli* accurately is the use of isotopic tracers. By making use of isotopic tracers, the opportunity is provided to track the behaviour of elements, for both *in vivo* and *in vitro* studies. Although iron has a great variety of radioactive isotopes,  $^{55}\text{Fe}$  ( $t_{1/2} = 2.74$  y) and  $^{59}\text{Fe}$  ( $t_{1/2} = 44.6$  y) can be considered the most suitable, because of their half-lives (Livechart – Table of Nuclides – Nuclear Structure and Decay Data, n.d.), and therefore provide various opportunities for the execution of tracer studies.

During this study,  $^{55}\text{Fe}$  is employed as a tracer.  $^{55}\text{Fe}$  mainly decays via electron capture (EC) to the ground state of  $^{55}\text{Mn}$ , as is shown in Figure 2 (Pommé et al., 2019); resulting in the emission of Auger electrons with low energies of 5.8 keV. Since the decay radiation can be considered as fairly low, Liquid Scintillation Counting (LSC) can be employed.

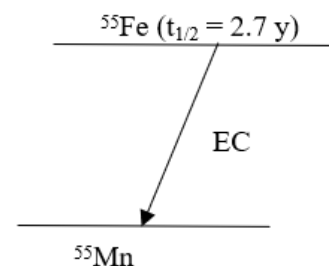


Figure 2. The decay scheme of  $^{55}\text{Fe}$ .

### 2.6. Methods for analysis

To both complement and confirm theoretical concepts, various analysis methods are available which can be employed in this research to draw further conclusions from performed experiments. Various methods have been chosen suitable to be employed, and in this section its most important characteristics will be elaborated shortly.

#### 2.6.1. X-ray diffraction

X-ray diffraction (XRD) can be employed to characterise crystalline materials. Since a variety of advantages can be ascribed to this method of analysis, it is used in several fields of research; e.g.

forensic sciences, geological applications, and the pharmaceutical industry (Bunaciu et al., 2015).

Figure 3 depicts a schematical representation in which the standard principles and instruments are included. X-rays are generated in a cathode ray tube, are filtered, collimated, and finally directed to the sample (Bunaciu et al., 2015). When the generated X-rays interact with the sample, and follows Bragg's law (Eq.5), constructive interference is produced.

$$n\lambda = 2d \sin \theta \quad (\text{Eq 5.})$$

In Eq.5,  $n$  is an integer,  $\lambda$  (nm) is the wavelength of the X-rays,  $d$  is interplanar spacing which generates the diffraction, and  $\theta$  ( $^\circ$ ) is the diffraction angle (Bunaciu et al., 2015).

Due to the interaction of the X-rays with the atoms in the material, intensity peaks will arise in specific directions (Stanjek & Häusler, 2004). For further improvement of signal-to-noise characteristics, a monochromator can be installed; this is preferable during the analysis of iron compounds (Bunaciu et al., 2015). Consequently, identification of the material is possible due to the conversion of the various intensity peaks to d-spacings, since each compound has a unique set of d-spacings (Bunaciu et al., 2015).

Bunaciu et al. (2015) mention three main advantages to the usage of XRD. Firstly, the method can be considered powerful for identifying unknown materials. Secondly, minimal sample preparation is necessary, making this method highly accessible in research. Finally, data can be interpreted relatively straightforward.

However, some limitations are also mentioned by Bunaciu et al. (2015); e.g. such as that the identification of unknown materials gives the most reliable results during the investigation of a homogeneous and single-phase material. Another limitation is that materials must be analysed in the form of a powder. Last but not least, one should have access to a database containing reference files for various inorganic compounds to identify the compound investigated.

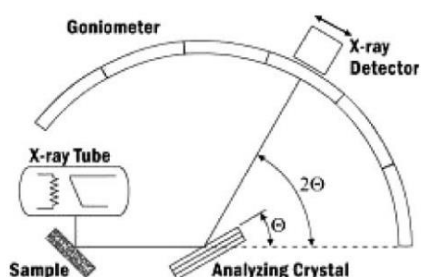


**Figure 3.** Diagram of a diffractometer system as employed in XRD. This figure is adapted from Bunaciu et al. (2015).

### 2.6.2. Liquid Scintillation Counting

A method which can be considered as being beneficial to detect a wide range of  $\alpha$  -and  $\beta$ -emitting radioisotopes is LSC. The technique is also highly applicable for low-activity measurements, as well

as for the detection of radioisotopes emitting lower energetic radiation. Since low-energy radiation has a short range, enabling fast absorption in e.g. the air or the sample itself, difficulties are encountered in detecting radiation of this kind. Hence, the usage of a scintillation cocktail is necessary to enable the transport of energy released through radiation and the emission of light (Gibson & Lally, 1971). A scintillation cocktail consists of an organic solvent and one or more fluor/scintillators. The solvent acts as an absorbent of the energy emitted by radioactive decay. The fluor/scintillator absorbs and re-emits the energy released by the solvent as visible light (PerkinElmer, n.d.-a).

### 2.6.2.1. Quenching

Despite the usage of a scintillation cocktail, not all energy emitted by a radioisotope is detected by the photomultiplier tube of the scintillation counter. This is called quenching. A variety of causes can be ascribed to this phenomenon. In Figure 4 a schematic representation of the liquid scintillation process, including the phenomenon of quenching, is depicted.

During a LSC measurement, quenching occurs due to three reasons. Firstly, when the scintillation cocktail and the sample containing the radionuclide are not properly homogenised, the radionuclide can be physically separated from the scintillation cocktail. This is known as physical quenching. Secondly, chemical quenching can occur when other compounds absorb the energy that is emitted by the radionuclide. As a result, less energy will reach the detector, reducing the number of counts. Lastly, colour quenching occurs when the emitted light is (partly) absorbed by the colour in the sample. Consequently, the detected light does not equal the actual amount of light emitted (PerkinElmer, n.d.-b).

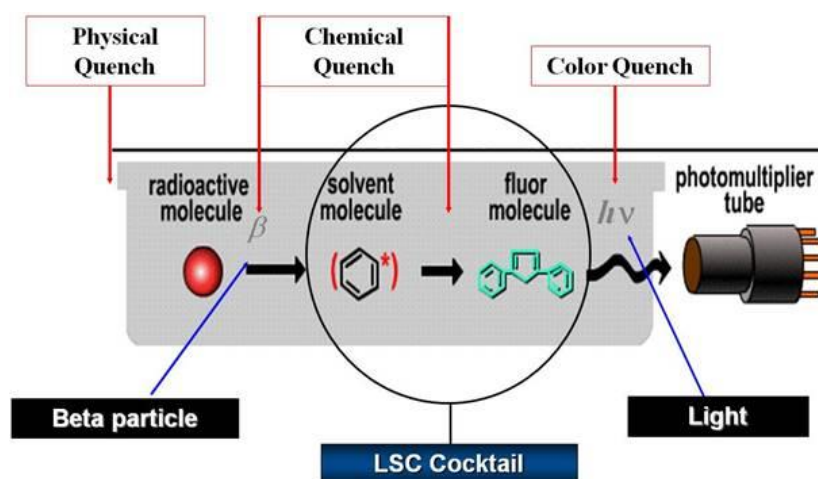


**Figure 4.** A schematic depiction of the various quenching forms in the liquid scintillation process. The figure is adapted from PerkinElmer (n.d.)

### 2.6.3. Inductively Coupled Plasma-Optical Emission Spectrometry

To determine the concentration of a specific chemical element in a sample, Inductively Coupled

Plasma-Optical Emission Spectrometry (ICP-OES) is highly suitable.

Figure 5 shows a schematic overview of the major components in ICP-OES systems. The two main components of the ICP-OES instrument are the plasma and the spectrometer. Plasma – such as argon – is used to excite atoms or ions. The plasma is introduced into the ICP torch, and a radiofrequency field is operated. As a result, a magnetic field is created, and the production of electrons and ions will start. The solution to be analysed is introduced into the system through the nebulizer. Since the produced electrons heat the plasma, the solution is converted into an aerosol. After deexcitation, light will be emitted by these atoms or ions, which is subsequently converted to an electrical signal (Sneddon & Vincent, 2008)

Transfer optics are employed to focus the emitted light on the spectrometer, where a photomultiplier tube (PMT) and other electronics subsequently convert the emitted light to an electrical signal. Since specific wavelengths correspond to specific atoms or ions, the concentration of an element can be deduced accordingly (Sneddon & Vincent, 2008). Further reading is recommended for an in-depth review of the various components of ICP-OES instruments and their function (Olesik, 1991; Sneddon & Vincent, 2008).

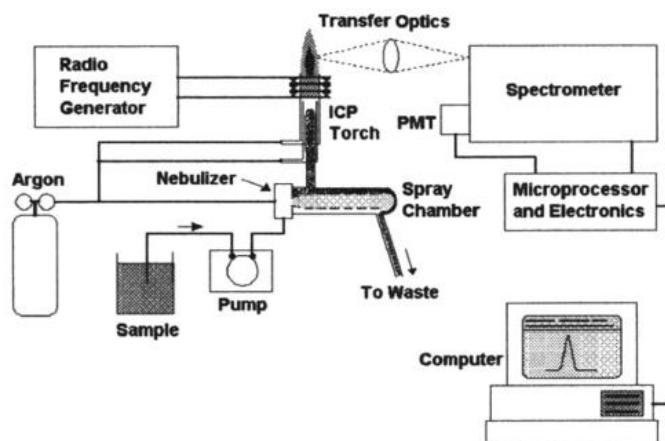


**Figure 5.** A schematic representation of an ICP-OES system. The main components are explained in section 2.6.3. This figure is adapted from Sneddon & Vincent (2008).

### 3. Materials & Methods

#### 3.1. Materials

*Table 3. List of chemical compounds.*

Chemical	Compound	Supplier	Specifications
Ascorbic acid	C <sub>6</sub> H <sub>8</sub> O <sub>6</sub>	Sigma-Aldrich	Powder
Bacto™ Tryptone	-	Gibco	Pancreatic Digest of Casein
Bacto™ Yeast extract	-	Gibco	Extract of Autolyzed Yeast Cells
Yeast extract	-	Oxoid	Extract of Autolyzed Yeast Cells
Fumaric acid	C <sub>4</sub> H <sub>4</sub> O <sub>4</sub>	Sigma-Aldrich	≥ 98%
Iron-55 Radionuclide	<sup>55</sup> FeCl <sub>3</sub>	PerkinElmer	74 MBq, ferric chloride in 0.5M HCl
Iron(II) chloride tetrahydrate	FeCl <sub>2</sub> x 4H <sub>2</sub> O	Supelco	For analysis, EMSURE, ACS, Reag. Ph. Eur.
Iron(III) chloride hexahydrate	FeCl <sub>3</sub> x 6H <sub>2</sub> O	Supelco	For analysis, EMSURE, ACS, Reag. Ph. Eur.
Sodium chloride	NaCl	Sigma-Aldrich	≥ 98%
Sodium hydroxide	NaOH	Sigma-Aldrich	Puriss. P.a., ACS reagent, reag. Ph. Eur., K ≤ 0.02%, ≥ 98%, pellets.
Sulphuric acid	H <sub>2</sub> O <sub>4</sub> S	Sigma-Aldrich	reag. ISO, reag. Ph. Eur 95-97%

*Table 4. List of products used*

Products	Characteristics
Eppendorf® tubes	Tube capacity 2 mL
Falcon culturing tubes	Gas-exchange lids, 50 mL volume.
Millex Syringe Filter	Millipore, 0.22 µm, used for sterilisation
Rotilabo®-Spritzenfilter	Nylon, 0.2 µm PA, Roth
Sapphire Pipette Tip 200 µL	Greiner Bio-One
Sapphire Pipette Tip 1000 µL	Greiner Bio-One
0.01 – 1 mL pipettes	Injekt®-F, Braun
20 mL High Performance Glass Vial	Used for Liquid Scintillation Counting, PerkinElmer
250 mL round-bottom flasks	-

*Table 5. List of instruments used*

Instruments	Specifications
Heater	Vos Instrumenten (VOS-12039)
Inductively Coupled Plasma-Optical Emission Spectroscopy	Optima 8000, PerkinElmer
Liquid Scintillation Counter	Tri-carb 2750TR/LL, Packard
Microcentrifuge	Micro star 17R, VWR
Orbital shaker	-
Spectrophotometer	Shimadzu, UV-1280
X-ray diffractometer	Philips PW0340 X'Pert PRO

### 3.2. Methods

#### 3.2.1. Synthesis of ferrous and ferric iron compounds

For this research, a selection of three salts – ferric sulphate, ferrous sulphate, and ferrous fumarate – were synthesised. To use the radioactive  $^{55}\text{Fe}$  as a tracer, which was only available in the form of ferric chloride, procedures were developed for their synthesis with ferric chloride as starting material.

##### 3.2.1.1. The synthesis of ferric sulphate

Firstly, ferric chloride was dissolved in MilliQ to make a solution of 0.11 M. This was followed by the addition of 18 M sulphuric acid in a volumetric ratio of ferric chloride solution to sulphuric acid of 9:1. After 30 minutes, the yellow-coloured solution was filtered through a nylon Rotilabo®-Spritzenfilter with a pore size of 0.2  $\mu\text{m}$  to remove unreacted iron particles. Two different experimental set-ups were tested. At first, the Erlenmeyer was placed directly onto the heater, as depicted in Figure 6. The temperature of the heating plate was set at 170°C. However, to pursue uniform heat distribution, in the second set-up shown in Figure 7, the Erlenmeyer containing the solution was placed in an oil bath where the temperature of the oil bath was monitored to be 170°C. For both set-ups, heating continued until the majority of liquid evaporated, and the white precipitate formed. In order to remove impurities, the precipitate was rinsed three times for 2 minutes with 5 mL acetone and left to dry overnight in the fumehood. This yielded a white crystal.

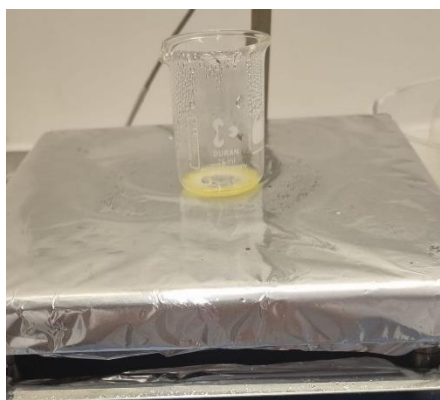


**Figure 6.** Set-up for the synthesis of ferric sulphate where the glasswork is directly placed onto the heater.



**Figure 7.** Set-up for the synthesis of ferric sulphate where the Erlenmeyer is placed into an oil bath. A thermometer was placed in the oil bath to monitor the temperature.

##### 3.2.1.1.1. Radiolabelling with $^{55}\text{Fe}$

The radioactive source containing  $^{55}\text{FeCl}_3$ , was brought into solution with MilliQ to yield a stock solution containing 1 MBq/100  $\mu\text{L}$ . This solution was used for further experiments.

In order to label ferric sulphate with  $^{55}\text{Fe}$ , 1 MBq of the stock solution was added to the yellow-coloured solution before filtration as described in section 3.2.1.1. Besides that the amount of added MilliQ was subtracted by 100  $\mu\text{L}$ , no further adjustments had been made with regard to the remaining steps of the synthesis as described in the previous section.

### *3.2.1.2. The synthesis of ferrous sulphate*

The main difference between the synthesis of ferric sulphate and ferrous sulphate is that during the latter, oxidation of iron(II) to iron(III) should be prevented and reduction of iron(III) to iron(II) should be achieved. This was tried to be achieved by primarily working under nitrogen atmosphere.

Firstly, a solution was made of 0.11 M ferric chloride in MilliQ. Afterwards, 18 M sulphuric acid was added in a volumetric ratio of 9:1 of ferric chloride solution to sulphuric acid. During these steps, a nitrogen atmosphere was created by the placement of a nitrogen (N<sub>2</sub>) inlet into the Erlenmeyer. The Erlenmeyer was covered at the top with Parafilm, and N<sub>2</sub>-gas was led into the Erlenmeyer using a plastic tube. After 30 minutes, the yellow-coloured solution was filtered through a Rotilabo®-Spritzenfilter (pore size 0.2 µm) in order to remove unreacted iron particles. The Erlenmeyer containing the filtered solution, was placed onto the heater in accordance to the set-up depicted in Figure 7. The oil-bath was kept at an temperature of 170°C. A nitrogen inlet was placed into the Erlenmeyer. Heating proceeded until the majority of liquid had evaporated, and the formation of a green-blue precipitate had started. By rinsing the precipitate three times with 5 mL acetone, impurities were removed. The precipitate was left to dry overnight in the fumehood.

#### *3.2.1.2.1. Ascorbic acid as a reducing agent*

To further enhance the possibility of reducing iron(III) to iron(II), ascorbic acid was used as a reductor. Additionally, a nitrogen atmosphere was created, and applied throughout the experiment, using the same method as described in the previous section.

After the addition of 18 M sulphuric acid to 0.11 M ferric chloride solution in a volumetric ratio of 9:1, ascorbic acid was added in a molar ratio to ferric chloride of 1:1. This yielded a colourless solution. This solution was filtered through a Rotilabo®-Spritzenfilter (pore size 0.2 µm) to remove unreacted iron particles. The temperature of the oil bath was monitored to be 70 °C, and the Erlenmeyer containing the colourless solution was placed within it. After 30 minutes, the solution coloured black, and heating was terminated. A black solution was yielded, and no precipitate was formed.

### *3.2.1.3. The synthesis of ferrous fumarate*

The synthesis of ferrous fumarate was based on the method described by Kapor et al. (2012). Firstly, sodium hydroxide was dissolved in MilliQ to yield a 2 M NaOH-solution. Fumaric acid was neutralised by the addition of 2 M NaOH-solution in a molar ratio of 1:2. The product of this neutralisation was disodium fumarate. Ferrous sulphate was added to disodium fumarate in a molar ratio of 1:1. The Erlenmeyer containing the solution of ferrous sulphate and disodium fumarate was placed in an oil bath according to the experimental set-up as depicted in Figure 7. In order to

prevent the oxidation of iron(II) to iron(III), the reaction was carried out in a nitrogen atmosphere. The nitrogen atmosphere was created similarly as described in section 3.2.1.2. The Erlenmeyer was placed in the oil bath for 25 minutes, with a temperature of the oil bath equal to 90°C. Impurities such as Na<sub>2</sub>SO<sub>4</sub>, FeSO<sub>4</sub>, and disodium fumarate, were removed by rinsing the precipitate three times with 5 mL MilliQ. Finally, the precipitate that was formed in the Erlenmeyer was dried at 105°C in the oil bath for 1 hour (Kapor et al., 2012).

### 3.2.2. Analysis

To confirm whether the syntheses were performed correctly, the obtained samples were analysed with XRD. For proper analysis, a minimum of approximate 0.10 gr of synthesised compound was needed. Sample preparation was executed by placing the desired amount of compound onto the spinner, dividing it equally over the surface of the spinner, and placing it in the diffractometer. The following settings were employed for the measurements:

- Scanning region between 5° and 90°.
- Scan step time of 400 seconds.
- Voltage of 45 kV.
- Current of 40 mA.
- A monochromator was used.
- Revolution time equal to two.

### 3.2.3. Preparation of iron supplementation solutions

#### 3.2.3.1. Non-radioactive ferrous sulphate solution

For the growth experiments where non-radioactive iron was supplemented, solutions were made of 3 and 30 µM. Firstly, 3 mmol of ferrous sulphate was dissolved in 100 mL MilliQ. 10 µL of this stock solution was added to 100 mL MilliQ to obtain the 3 µM ferrous sulphate solution, whereas for 30 µM, 100 µL was added to 100 mL MilliQ. Afterwards, sterilisation was done by pipetting the solutions through a 0.22 µm Millex sterilisation filter.

#### 3.2.3.2. Non-radioactive ferric sulphate solution

Ferric sulphate solutions of 3 and 30 µM were prepared similarly as described in the previous section. A stock solution was made by dissolving 3 mmol ferric sulphate in 100 mL MilliQ. Respectively, 10 and 100 µL were added to 100 mL MilliQ to obtain 3 and 30 µM ferric sulphate solutions. The solutions were sterilised through a 0.22 µm Millex sterilisation filter.

#### 3.2.3.3. Radiolabelled ferric chloride solution

Since the radionuclide <sup>55</sup>Fe was available in the form of ferric chloride, this form of iron was chosen to perform growth experiments with. Two different concentrations were selected for supplementation: 3 and 30 µM. Firstly, a stock solution was made by dissolving 3 mmol of ferric chloride in 100 mL MilliQ. For the 3 and 30 µM solution, respectively 10 and 100 µL were pipetted out of the stock

solution and added to 100 mL MilliQ. Afterwards, 0.1 MBq of  $^{55}\text{FeCl}_3$ -solution was added to both solutions. The amount of iron in 0.1 MBq of  $^{55}\text{FeCl}_3$ -solution was considered negligible. At last, a 0.22  $\mu\text{m}$  Millex sterilisation filter was used to sterilise the solutions.

#### 3.2.3.4. Radiolabelled ferric sulphate solution

For ferric sulphate supplementation, equal concentrations of 3 and 30  $\mu\text{M}$  were chosen as for ferric chloride. At first, 0.36 mmol of radiolabelled ferric sulphate – synthesised as described in section 3.2.1.1.1. – was dissolved in 100 mL MilliQ to make a stock solution. For the 3  $\mu\text{M}$  solution, 1 mL of the stock solution was added to 99 mL of MilliQ, whereas for the 30  $\mu\text{M}$  solution, 10 mL was added to 90 mL of MilliQ. Finally, the solutions were sterilised through a 0.22  $\mu\text{m}$  Millex sterilisation filter.

#### 3.2.4. Culturing of *Escherichia coli*

##### 3.2.4.1. Preparation of plate cultures of *Escherichia coli*

To reduce repeated exposure of the *E.coli* K12 stock, agar plate cultures were prepared. In addition, the preparation of plate cultures gave rise to the opportunity to inoculate single colonies. After preparing the agar plates, consisting of Luria-Bertani (LB) agar, the plates were streaked with the liquid *E.coli* K12 culture. The plates were incubated at 37°C in a stationary incubator for 16-18 hours. Afterwards, the plates were stored in a fridge at ca. 5°C.

##### 3.2.4.2. Preparation of Luria-Bertani broth

LB broth was chosen as a growth medium for *E.coli* since it is most commonly used, and has characteristics that promote fast growth while yielding good plasmids (Lessard, 2013).

Bactotryptone (10 g), Bacto™ Yeast extract / Yeast extract (5 g), and sodium chloride (10 g) were dissolved in 1000 mL MilliQ. Afterwards, the pH was measured and adjusted when necessary to  $\text{pH } 7.2 \pm 0.2$  using a 5 M NaOH-solution (Lessard, 2013). The solution was distributed to 4 Schott bottles, each containing 250 mL solution. The 4 Schott bottles containing LB-medium were sterilised by autoclaving for 15 minutes at 121°C.

##### 3.2.4.2.1. Analysis

Since the LB broth could be prepared with either Bacto™ Yeast (Gibco) extract or Yeast extract (Oxoid), the difference between the two was determined for the accuracy of the results. Therefore, the iron concentrations of both preparations were measured with ICP-OES. For sample preparation, 1 mL of LB-medium was dissolved in 9 mL MilliQ. Dilution was deemed necessary since LB-medium contains sodium chloride.

##### 3.2.4.3. Growth curve experiments

For each growth curve experiment, a preculture was prepared the day prior by inoculating approximately 10 mL of LB broth in a 50 mL round-bottom flask with a single colony of plated *E.coli*. The liquid culture was incubated in an orbital shaker for 16-18 hours at 37°C and 180 rpm. Inoculation was performed in a 250 mL round-bottom flask, with a dilution factor equal to a hundred. Each growth

curve experiment was performed in duplo. In addition, the experiment was performed 'blanco', meaning no iron was supplemented; therefore, reflecting the unmodified growth of the organism.

#### 3.2.4.3.1. Applying the logistic model

The construction of regression curves enabled estimating the three growth parameters. For this analysis, Ordinary Least-Squares (OLS) had been chosen as the regression method as described in section 2.4.1.2.1.1.

#### 3.2.4.3.2. Non-radioactive iron supplementation

To determine whether iron supplementation would have no harmful effect on the growth of *E.coli*, firstly experiments were conducted where non-radioactive iron was supplemented. Iron supplementation was performed with both ferrous and ferric sulphate in concentrations of either 3 or 30  $\mu\text{M}$ . The LB-medium that was used consisted of the ingredients listed in section 3.2.4.2., where Bacto™ Yeast extract was used.

Culturing of *E.coli* was performed in 50 mL sterilised disposable Falcon tubes where 5 mL of *E.coli* - inoculated as described in section 3.2.4.3 – was pipetted into a Falcon tube. For each time point, a separate Falcon tube was employed. After preparing the blanco data set, iron was supplemented to the remaining inoculated medium in a ratio of 1:10. Afterwards, the Falcon tubes were filled in duplo with 5 mL of the iron-supplemented inoculated medium. The Falcon tubes were simultaneously put in the orbital shaker for 1-24 hours.

For the construction of a growth curve, twelve time points were taken from  $t = 0$  h to  $t = 24$  h. At each of these timepoints, one Falcon tube of the blanco data set, and two Falcon tubes with iron supplementation were taken out of the orbital shaker. The second column ( $\mu\text{L inoculated medium}$ ) of Table 6 shows the amounts of the inoculated medium that was pipetted out of each Falcon tube into a 1.5 mL cuvette for each time point. The values that are depicted in the last column ( $\mu\text{L LB-medium}$ ) of Table 6 are equal to the amounts of LB-medium that were added to the 1.5 mL cuvettes containing the inoculated medium. The cuvettes were placed into the spectrophotometer at room temperature, and OD measurements were performed at 600 nm. The absorbance was measured with respect to the value of unmodified LB-medium.

#### 3.2.4.3.3. Radionuclide iron supplementation

For the growth curve experiments where *E.coli* was supplemented with radiolabelled  $^{55}\text{Fe}$ , culturing was performed in sterilised 250 mL round-bottom flasks due to scarcity of the Falcon tubes. Firstly, for blanco measurements, 25 mL of inoculated medium – as described in section 3.2.4.3. – was pipetted into three round-bottom flasks. Secondly, either ferric chloride solution (3 or 30  $\mu\text{M}$ ) or radiolabelled ferric sulphate solution (3 or 30  $\mu\text{M}$ ) was pipetted into the inoculation flask in a ratio of 1:10. Afterwards, 25 mL of the iron-supplemented inoculated medium was pipetted in three round-bottom flasks in duplo. A total of nine round-bottom flasks was put in an orbital shaker for a

maximum period of time of 24 hours at 37°C and 180 rpm.

For the construction of a growth curve, the values depicted in the second column ( $\mu\text{L}$  inoculated medium) of Table 6 were pipetted out of the round-bottom flasks into an 1.5 mL cuvette. The inoculated medium was diluted when necessary with the amounts of LB-medium as depicted in the last column ( $\mu\text{L}$  LB-medium) of Table 6. The cuvette was placed into the spectrophotometer, and the OD was measured at 600 nm at room temperature pertaining to the value of unaltered LB-medium.

**Table 6.** The required amounts of inoculated medium and LB-medium to obtain correct  $\text{OD}_{600}$  measurements. These values change throughout the growth experiment, since it was aimed to stay obtain values from the spectrophotometer between 0 and 0.6 AU. Higher values would compromise the validity and certainty of the measurements. To correct for the dilution, the value measured by the spectrophotometer was multiplied with the dilution factor. For the growth experiments were radiolabelled  $^{55}\text{Fe}$  was supplemented, it is shown how many medium is extracted of a flask throughout the experiment. After  $t=3$ , extraction of the inoculated medium was done from flask 2, in order to avoid the influence of decreasing amount of medium present for the organism to grow on.

Timepoint (h)	$\mu\text{L}$ inoculated medium	$\mu\text{L}$ LB-medium
<b>Flask 1</b>		
t = 0	1000	0
t = 1	1000	0
t = 2	1000	0
t = 2.5	1000	0
t = 3	1000	0
<b>Flask 2</b>		
t = 3.5	500	500
t = 4	500	500
t = 4.5	500	500
t = 5	250	750
t = 5.5	250	750
t = 6	250	750
<b>Flask 3</b>		
t = 24	100	900

After the  $\text{OD}_{600}$  measurements were performed at each time point, the 1 mL was pipetted out of the cuvette, and transferred to an Eppendorf tube. The Eppendorf tube was centrifugated at 2000 rpm for 2 minutes. The bacteria were found at the bottom of the Eppendorf tube, whereas the remaining LB-medium could be found on the top. The latter was pipetted in another Eppendorf tube. The tubes were stored in the freezer at -18°C until further measurements were performed.

### 3.2.5. Liquid Scintillation Counting as a method of analysis

In order to determine the iron uptake of *E.coli*, the contents of the Eppendorf tubes, which consistency is elaborated upon in the previous section, were analysed with LSC for each time point to determine the amount of  $^{55}\text{Fe}$  that was still present in the medium.

### *3.2.5.1. Sample preparation*

To determine what amount of LB-medium should be added to the scintillation cocktail, while still measuring with sufficient efficiency, a calibration curve was made as described in Appendix C. 10 samples were made with equal amounts of activity, while varying the amount of LB-medium added; ranging from 0.1 mL to 1 mL. For further experiments, 0.5 mL of the samples obtained in section 3.2.4.3.3., was added to 19.5 mL of the scintillation cocktail. Since this created a two-phased system, the vials were shaken thoroughly by hand for approximately ten seconds, until complete dispersion was achieved. Before starting the measurement, the vials were put in the LSC for half an hour to prevent excitation due to light influencing the measurements.

### *3.2.5.2. Settings Liquid Scintillation Counter*

The following settings were employed for the measurements:

- Counting time of 30 minutes.
- Quench indicator tSIE was used.
- No half-life corrections were made.
- Measurements were done in three regions:
  - Region A: 0.0 – 6.0 keV
  - Region B: 2.0 – 6.0 keV
  - Region C; 6.0 – 2000 keV
- The results obtained in region A were used for further analysis.

## 4. Results and discussion

### 4.1. Synthesis of ferrous and ferric compounds

#### 4.1.1. Synthesis of ferric sulphate

Firstly, ferric sulphate was synthesised. Throughout the process of optimising the synthesis method, two different heating set-ups were evaluated as depicted in Figure 6 and 7. Despite prolonging the duration of heating for the latter set-up upto twice the time required for the set-up of Figure 6, no precipitate was formed. Therefore, the set-up of Figure 6 was preferred over the one of Figure 7. It should be taken into account that in the oil bath a magnetic stirrer was placed to acquire uniform heat distribution. Despite that magnetical stirring has been employed frequently in research, mechanical stirring could be more suitable to prevent aggregation of magnetic species (Kansara et al., 2018; Podgórna & Szczepanowicz, 2016; Souza et al., 2007). Since ferric chloride and ferric sulphate contain paramagnetic characteristics, aggregation of these species could have hindered the crystallisation process.



**Figure 8.** White precipitate which was yielded following the procedure as described in section 3.2.1.1.

In order to confirm whether the synthesis had been performed correctly, an XRD-spectrum was taken; of which the results are shown in Figure 9. As is depicted in Figure 9, similar peaks are visible between the peaks from the synthesised compound, and the data of the software for XRD-analysis. The compound was matched by the Highscore Plus software to the database of the International Centre for Diffraction Data (ICDD) to be hydrogen ferric sulphate hydrate with a match score of 85.

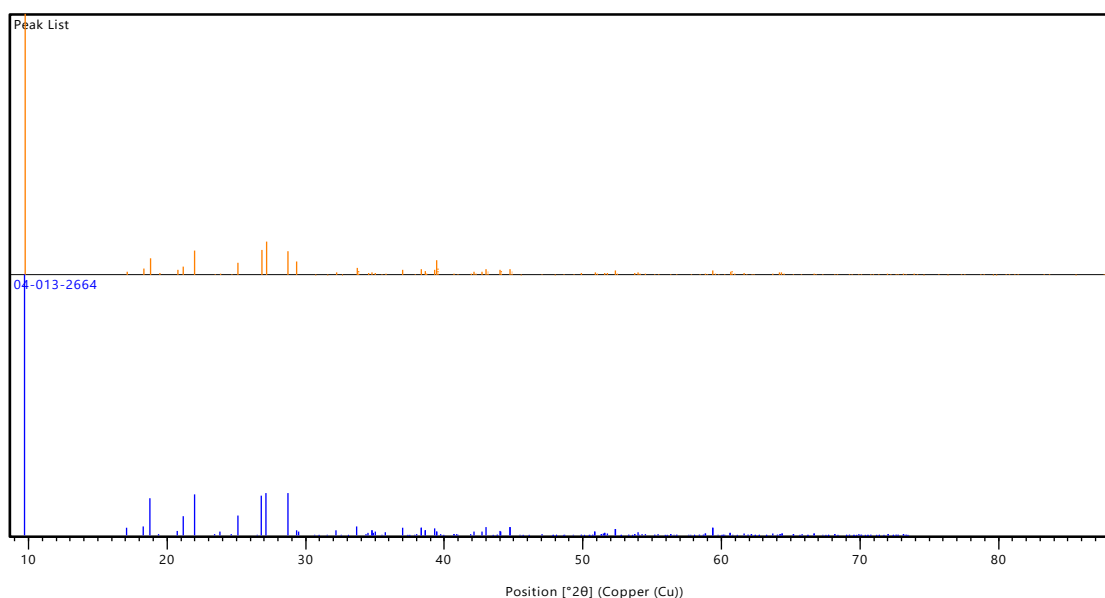


**Figure 9.** XRD-spectrum of hydrogen ferric sulphate hydrate. The orange-coloured spectrum at the top is obtained from the XRD-measurement of the synthesised compound. The lower blue-coloured spectrum is the spectrum in the ICDD database that is used for identification of the synthesised compound.

#### 4.1.1.1. Radiolabelling of ferric sulphate

After the synthesis of ferric sulphate had been optimized, the compound was radiolabelled. Based on both the optimization of the procedure, and the visual similarity between the non-radiolabelled compound and the radiolabelled compound, it was assumed that the radiolabelling had been executed correctly, and did not affect the composition of the compound. This assumption has been made due to time constraints. However, it is preferred to analyse the sample prior to confirm whether it was synthesised correctly.

#### 4.1.2. Synthesis of ferrous sulphate

Secondly, the synthesis of ferrous sulphate was conducted as described in section 3.2.1.2. However, difficulties were encountered with regard to the oxidation of iron(II) to iron(III). Although the synthesis was executed under a nitrogen atmosphere, reduction from iron(III) to iron(II) does not happen spontaneously. Resultingly, the white-coloured crystal ferric sulphate was yielded instead of the desired blue-green ferrous sulphate.

In order to reduce iron(III) to iron(II), an experiment has been conducted where the reducing agent ascorbic acid was included in the synthesis. The latter had been chosen as a reducing agent, since studies have reported that it functions as a reducing agent in the human body (Abbaspour et al., 2014; Stoffel et al., 2020; Yilmaz & Li, 2018). Additionally, a study had been conducted where ascorbic acid successfully reduced iron(III) (Elmagirbi et al., 2012). Therefore, ascorbic acid was added in a molar ratio to ferric chloride of 1:1. However, during heating, the solution coloured black, and no crystallization occurred. This could be explained by the fact that the reducing properties of ascorbic acid were maximized when executed in a solution where the pH ranges from 1-4, whereas the experiment in this study was conducted around a pH of 7 (Elmagirbi et al., 2012).

Since repeated execution of the experiment as described in section 3.2.1.2. did not yield the expected results, it was examined whether the procedure for the synthesis of ferrous sulphate did succeed when the reduction of iron(III) to iron(II) could be prevented by employing ferrous chloride as the starting material. The steps for this experiment were conducted exactly under the same conditions as those reported in section 3.2.1.2. During heating, a green-blue precipitate was formed, which can be expected to be ferrous sulphate. However, after removal of the nitrogen inlet to rinse the precipitate with acetone, the precipitate oxidized immediately; yielding a yellow-brown substance. As a result, no ferrous sulphate had been synthesised successfully, and therefore ferrous sulphate was excluded from executing further experiments such as radiolabelling, and growth experiments.

#### 4.1.3. The synthesis of ferrous fumarate

Finally, the procedure for the synthesis of ferrous fumarate was conducted as described in section 3.2.1.3, yielding a brick-red precipitate as depicted in Figure 10. In reported previously performed research, a similar colour was



**Figure 10.** Brick-red precipitate which was yielded following the procedure as described in section 3.2.1.3.

observed (Kapor et al., 2012). In order to determine whether the obtained compound was indeed ferrous fumarate, XRD-analysis had been conducted. This resulted in the XRD-spectrum as depicted in Figure 11. The upper spectrum shows the peaks that are obtained from the synthesised compound. Similar peaks are found in the spectrum in the ICDD database as depicted in the lower part of Figure 11. The Highscore Plus software matched the peaks from the synthesised compound and the data of the ICDD database to be ferrous fumarate,  $C_4H_4FeO_4$ , with a score of 80. Therefore, it can be concluded that ferrous fumarate had been synthesised correctly.

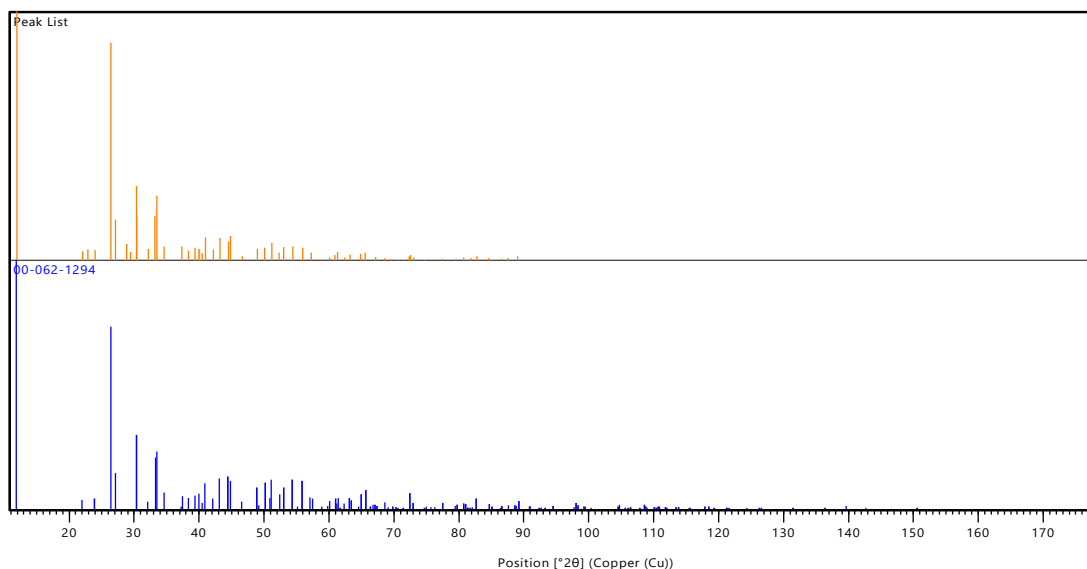


**Figure 11.** XRD-spectrum of ferrous fumarate. At the top, the orange-coloured spectrum is shown that is obtained from the XRD-measurement of the synthesised compound. The lower blue-coloured spectrum is the spectrum in the ICDD database that is used for further identification of the synthesised compound.

#### 4.1.3.1. Radiolabelling of ferrous fumarate

However, despite the successful synthesis, radiolabelling of ferrous fumarate with  $^{55}Fe$  could not be executed. As discussed in section 4.1.2, the synthesis of ferrous sulphate was unsuccessful. Therefore, radiolabelled ferrous sulphate could not be employed as the starting material for ferrous fumarate. Resultingly, ferrous fumarate was excluded for executing further experiments.

### 4.2. Growth curve experiments of *Escherichia coli*

#### 4.2.1. Luria-Bertani broth

As described in section 3.2.3.2., Luria-Bertani broth could be either synthesised with Bacto™ Yeast Extract (Gibco) or Yeast Extract (Oxoid). In order to investigate whether there were any differences between the two, ICP-OES was employed to determine the iron concentration of the two preparations. The results are shown in Table 7.

Ingredient	Iron concentration (mg/L)	Concentration (M)
Bacto™ Yeast Extract (Gibco)	0.026	4.66 x 10 <sup>-7</sup>
Yeast Extract (Oxoid)	0.0	0.0

Table 7. ICP-OES results of LB-broth.

During the growth experiments that were conducted using non-radioactive iron supplementation, LB broth was used with Bacto™ Yeast Extract. Despite the fact that there was aimed to conduct growth experiments for both radioactive and non-radioactive iron supplementation with equal broth compositions, Yeast Extract from Oxoid was employed for the latter, due to a change of supplier. Tachibana et al. (2021), have investigated the differences in cell yield of *E.coli* of various yeast extracts relative to Bacto™ Yeast Extract. The composition of different brands of yeast extract did influence the cell yield of *E.coli* (Tachibana et al., 2021). Although the Yeast Extract from Oxoid was not investigated in this research, the difference in iron concentration indicates that there are indeed variations between yeast extract compositions. In addition, it has been reported that the composition of LB-broth differs from batch to batch, and variations that occur with the age of each batch due to the degradation of amino acids through exposure to light (Sezonov et al., 2007). Therefore, differences regarding cell growth of *E.coli* could be ascribed to LB-medium, and were expected in the growth experiments.

#### 4.2.2. Construction of the growth curves

##### 4.2.2.1. Growth of *E.coli* on Luria Bertani broth with Bacto™ Yeast Extract

The mean growth behaviour of *E.coli* on unmodified LB-medium is depicted in Figure 12. From the regression function, (section 3.4.1.1.2), estimations have been made with regard to the three growth parameters, resulting in Eq 6. as the non-linear regression function. For the regression, the best fit was obtained with non-weighting regression, since it fitted the growth curve the best. Research has shown that regressions executed with different weighting methods yielded similar results, and thus there was chosen to report using non-weighted regression (McKellar et al., 2014).

$$OD_{600} = \frac{2.25}{(1+e^{-0.666 \times (t-4.20)})} \quad (\text{Eq.6})$$

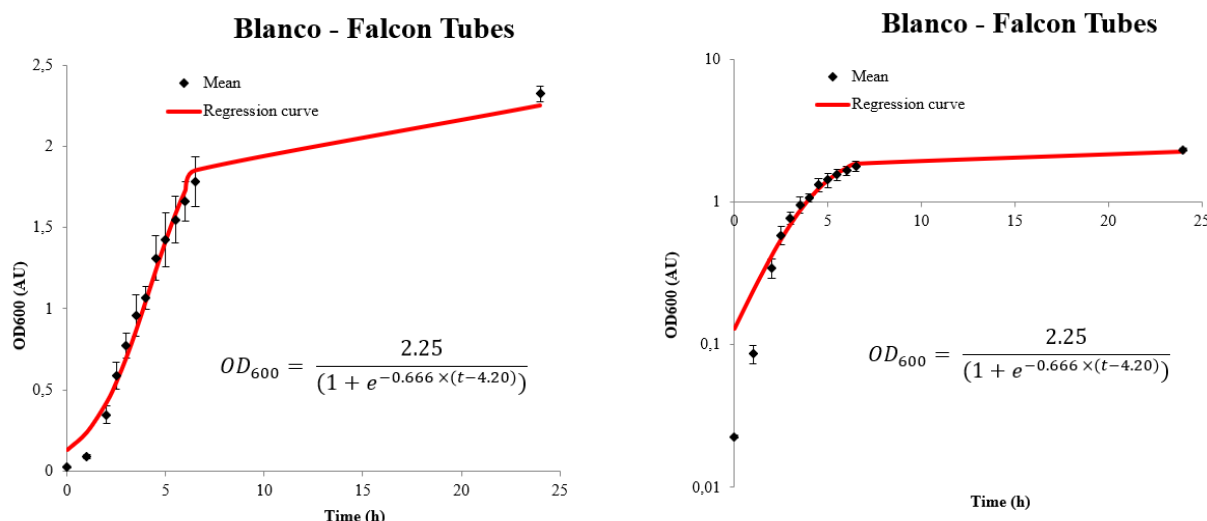


**Figure 12.** Mean growth behaviour of *E. coli* on LB-medium containing Bacto™ Yeast Extract. Growth experiments were performed in 50 mL Falcon tubes. The mean (left) and log-scale (right) growth curves were fitted by OLS.

#### 4.2.2.1.1. The impact of non-radioactive iron supplementation

In order to investigate the influence of supplementation of a variety of iron compounds to *E. coli*, and whether the supplementation would not have detrimental effects on the viability of an *E. coli* colony, at first experiments were performed where non-radioactive iron was supplemented in either the form of ferrous sulphate or ferric sulphate. In addition, the supplementation of these compounds could provide insights into possible differences between ferrous and ferric iron regarding growth of *E. coli*.

In Appendix A, the results of the growth curve experiments can be found for the supplementation of ferrous sulphate and ferric sulphate (3 and 30  $\mu\text{M}$ ). The estimations for the different growth parameters that are obtained from the regression curve are summarized in Table 8.

Conditions	OD <sub>600,max</sub> (AU)	$\mu_{\text{max}}$ (h <sup>-1</sup> )	t <sub>i</sub> (h)	n
LB (Bacto™ Yeast Extract)	2.25	0.666	4.20	7
3 $\mu\text{M}$ ferrous sulphate	2.06	0.961	3.70	2
30 $\mu\text{M}$ ferrous sulphate	2.15	0.845	3.80	2
3 $\mu\text{M}$ ferric sulphate	1.96	0.906	3.53	2
30 $\mu\text{M}$ ferric sulphate	2.08	0.865	3.68	2

**Table 8.** The estimated growth parameters were obtained from the regression curves as depicted in Appendix A.

The initial OD<sub>600</sub>-value (AU) can be considered a reflection of the cell density at the beginning of a growth experiment. For the blanco experiment this value was measured to be  $0.023 \pm 0.006$ . After iron supplementation, the initial OD<sub>600</sub>-value (AU) was measured to be similar to that of growth on unmodified LB-medium, with a value of  $0.019 \pm 0.002$  AU. Therefore lying between the standard deviation (SD) interval. This indicates comparable starting conditions for the conducted growth experiments.

Various differences can be observed between the growth parameters of the blanco experiment and that of iron supplementation. Firstly, an increase of the maximum specific growth rate ( $\mu_{\text{max}}$ ) of a

minimum of 26% was achieved. The addition of only 3  $\mu\text{M}$  of either ferrous or ferric sulphate resulted in an increase of  $\mu_{\text{max}}$  of at least 36%. This indicates that the LB-medium is iron-deficient which has been confirmed by the ICP-OES results depicted in Table 7. Therefore, supplementation of 3  $\mu\text{M}$  of either ferrous or ferric sulphate already provides *E.coli* with better growing conditions. In previous research, the supplementation of small concentrations of iron has been shown to improve the growth of *E.coli* as well (Hartmann & Braun, 1981).

The maximum cell densities that have been achieved with iron supplementation have been consequently lower in comparison to the blanco measurements. Additionally, the lower values that have been estimated for the inflection point,  $t_i$ , are indicative that the exponential phase lasts shorter in comparison to the blanco measurements. Research has shown that the exponential phase of *E.coli* on LB-broth ends at an  $\text{OD}_{600}$ -value of approximately 0.3 AU, which is followed by a period of time where the growth rate decreases gradually (Sezonov et al., 2007). The growth curves depicted in Figure 12 and Appendix A are in accordance with the findings of Sezonov et al. (2007). Combining the estimated increase of the  $\mu_{\text{max}}$  with the estimated expedited inflection point, it seems that, although iron-supplemented *E.coli* grows faster, it does not maintain this situation for a long period of time. Ratledge & Winder (1964) have shown that increments in the amount of iron supplementation led to an increase in  $\mu_{\text{max}}$ , whereas the time of the exponential phase decreased. However, Ratledge & Winder (1964) reported an increase in cell yield under these circumstances, whereas in this study lower values for the  $\text{OD}_{600,\text{max}}$  are estimated during iron supplementation, indicating that cell yield are lowered. Since this was not expected based on literature, this could be indicative that other factors may be considered growth-limiting.

#### 4.2.2.2. Growth of *E.coli* on Luria Bertani broth with Yeast Extract

The mean growth behaviour of *E.coli* on LB-medium with yeast extract is depicted in Figure 13. For the experiments discussed in section 3.2.4.3.3., 250 mL round-bottom flasks were used.

From the regression function, the three growth parameters could be estimated, resulting in Eq 7. as the non-linear regression function. Non-weighted regression was chosen since the regression curve fitted the growth curve properly. Additionally, research has shown that the results with different weighting factors yielded similar values for the growth parameters (McKellar et al., 2014). Therefore, no weighting was employed during the construction of the regression functions.

$$\text{OD}_{600} = \frac{1.51}{(1+e^{-1.61 \times (t-3.00)})} \quad (\text{Eq.7})$$

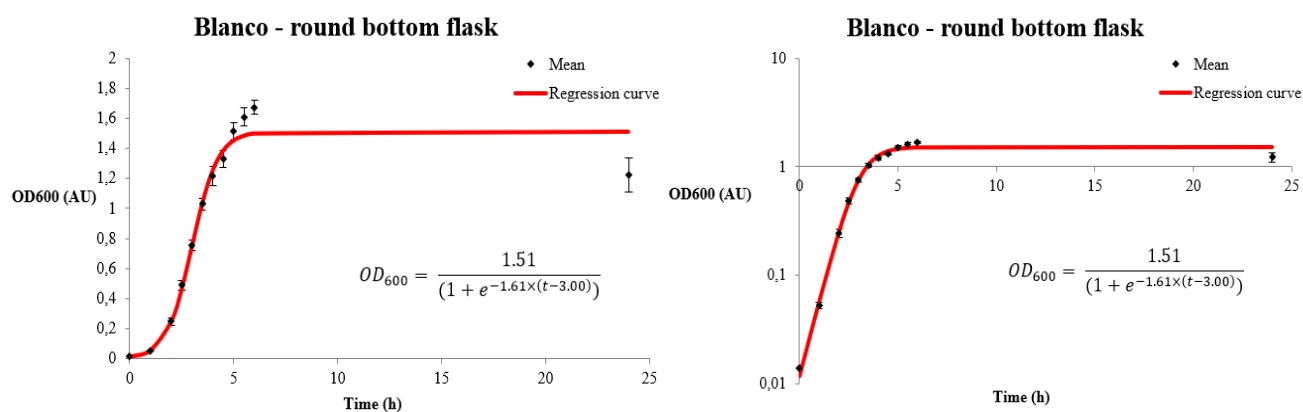


**Figure 13.** Mean growth behaviour of *E. coli* on LB-medium containing Yeast Extract (Gibco). Growth experiments were performed in 250 mL round-bottom flasks.. The mean (left) and log-scale (right) growth curves were fitted by OLS.

#### 4.2.2.2.1. Supplementation with the radiolabelled $^{55}\text{Fe}$

In Appendix B, the results of the growth curve experiments can be found for the supplementation of radiolabelled ferric chloride and ferric sulphate (3 and 30  $\mu\text{M}$ ). The estimations for the different growth parameters obtained from the regression curves are summarised in Table 9.

**Table 9.** The estimated growth parameters which have been obtained from the regression curves as depicted in Appendix B.

Conditions	$\text{OD}_{600,\text{max}}$ (AU)	$\mu_{\text{max}}$ ( $\text{h}^{-1}$ )	$t_i$ (h)	n
LB (Yeast extract)	1.51	1.61	3.00	4
3 $\mu\text{M}$ $^{55}\text{FeCl}_3$	1.37	1.69	2.87	2
30 $\mu\text{M}$ $^{55}\text{FeCl}_3$	1.40	1.72	2.97	2
3 $\mu\text{M}$ $\text{H}^{55}\text{Fe}(\text{SO}_4)_2 \times 4\text{H}_2\text{O}$	1.46	1.66	2.93	2
30 $\mu\text{M}$ $\text{H}^{55}\text{Fe}(\text{SO}_4)_2 \times 4\text{H}_2\text{O}$	1.34	1.52	2.97	2

The cell densities at the beginning of the growth experiments can be compared to evaluate whether the starting conditions can be considered as being similar. For the blanco experiment the  $\text{OD}_{600}$ -value (AU) was measured to be  $0.014 \pm 0.0008$ . After iron supplementation with ferric chloride, the initial  $\text{OD}_{600}$ -value (AU) was measured to lie inside the SD interval, whereas iron supplementation with ferric sulphate resulted in values slightly outside the SD interval. This indicates similar starting conditions for ferric chloride iron supplementation, whereas for ferric sulphate iron supplementations these can be considered slightly less similar. However, since it is reported that bacterial growth is not dependent on prior nutrient storage in the cells of the organism, it was expected that iron utilization will not be affected due to lower starting cell densities (Appenzeller et al., 2005).

In comparison to the estimated growth parameters of the blanco measurements, the growth parameters obtained with iron supplementation differ slightly. With regards to the value of  $\mu_{\text{max}}$ , a minimum increase of 3.1% is observed. In addition, a small increase in the value of  $\mu_{\text{max}}$  is observed between 3 and 30  $\mu\text{M}$  ferric chloride supplementation. Similar results have been reported by Hartmann & Braunn (1981) and Ratledge & Winter (1964). However, the supplementation of 30  $\mu\text{M}$  ferric

sulphate induces a negative effect on the growth rate, leading to a decrease of the value of  $\mu_{\max}$  of 5.6%. These results were not expected based on previous research, and therefore it could be suggested that other factors influence the growth of *E.coli*.

Additionally, a decrease is observed for the estimated value of  $OD_{600, \max}$ . However, the mean  $OD_{600}$ -value (AU) at the end of the blanco experiment ( $t=24$ ) is  $1.22 \pm 0.12$ , comprising the region in which the final  $OD_{600}$ -values lie for iron-supplemented experiments. From the figures that are depicted in Appendix B, a slightly shorter exponential phase is observed. This is confirmed by the estimated value for  $t_i$ , which is lower than the value of 3.00 h estimated for the blanco measurements. This is in accordance with the results reported in previous research (Hartmann & Braun, 1981; Ratledge & Winder, 1964).

#### 4.2.2.3. Comparison of the growth experiments

Despite it being preferred to investigate non-radioactive and radioactive iron supplementation under the same growth conditions, 250 mL round-bottom flasks were chosen for the latter due to scarcity of the 50 mL Falcon tubes. However, to evaluate whether the starting conditions were similar for both Falcon tube and round-bottom flask blanco measurements, the value of  $OD_{600}$  at the first timepoint ( $t=0$ ) has been compared. The value for the growth experiments in Falcon tubes was found to be  $0.023 \pm 0.006$ , whereas for the round-bottom flasks a value was found of  $0.014 \pm 0.0008$ . Therefore, in the latter experiments, lower cell densities were started with.

When considering the final  $OD_{600}$ -value ( $t=24$ h), different results were yielded than expected. As depicted in the left graph of Figure 13, the  $OD_{600}$ -value (AU) at  $t=24$  lies far below the regression curve. This is also depicted in Figures B-1 – B-4 in Appendix B. Where an asymptotic graph was expected, the results led to a steep decrease. Therefore, based on the final  $OD_{600}$ -value ( $t=24$ h) of the growth experiments, it is suggested that the colonies of *E.coli* in flask 3 were not viable anymore. Throughout the growth experiments of radionuclide iron supplementation, the experimental conditions were kept equal, including the placement of the various flasks in the incubator. These flasks were consistently placed at the back of the incubator, close to the heating element, and thus possible higher temperatures were reached than the optimal growth temperature of *E.coli* of 37°C. Noor et al. (2014) have reported drastically suppressed the growth of *E.coli* at LB-medium at higher temperatures (45°C) in comparison to the optimal temperature of 37°C. Therefore, the cell death that has been observed throughout the growth experiments could be ascribed to possible higher temperatures that have been reached in these flasks due to their placement in the incubator. During the growth experiments conducted with non-radioactive iron supplementation, the Falcon tubes were placed on the sides of the incubator, whereas the heating element was placed in the back.

A striking difference was observed during the comparison of the growth parameters of *E.coli* in 50 mL Falcon tubes to the growth in 250 mL round-bottom flasks. Firstly, for the value of  $\mu_{\max}$ , an increase of 142% was found compared to the measurements in the 50 mL Falcon tubes. Higher growth

rates were expected since the round-bottom flasks are larger, contain five times more medium than the Falcon tubes, and the surface available for gas-exchange is higher. Despite that LB-medium with Bacto™ Yeast Extract contained a small concentration of iron, the growth was significantly limited in comparison to the LB-medium with Yeast Extract (Gibco). This could be indicative that iron could possibly not be considered the main factor limiting the growth of *E.coli*, whereas e.g. gas-exchange surface, or size of the culturing flasks could be.

The results of the experiments with radiolabelled iron supplementation seem to be in accordance with the last-mentioned indication. With regards to the supplementation of ferric chloride, a small increase of the estimated value of  $\mu_{\max}$  was observed between 3 and 30  $\mu\text{M}$ , which was expected based on previous research (Hartmann & Braun, 1981). However, regarding the supplementation of ferric sulphate, a relative decrease of 8.6% was observed for the estimated value of  $\mu_{\max}$  for 30  $\mu\text{M}$  supplementation compared to 3  $\mu\text{M}$  supplementation. Therefore, it can be stated that higher concentrations can not always be considered as being advantageous for the pathogen, leading to the question of which conditions can be accounted for as being growth limiting.

The size of different growth vessels has been investigated in previous research on *Staphylococcus aureus* (van Dijk, 2021). No significant differences were observed between culturing in 50 mL Falcon tubes or 250 mL round-bottom flasks. However, this may not be the case for *E.coli*. In addition, growth in LB-broth is limited by the availability of carbon sources, and amino acids present in LB-broth are depleted throughout time, possibly influencing the growth of the organism as well (Sezonov et al., 2007).

#### 4.3. Liquid Scintillation Counting

Throughout the experiments,  $^{55}\text{Fe}$  has been employed as a tracer to investigate the behaviour *E.coli* in relation to the uptake of 3 and 30  $\mu\text{M}$  iron supplementation of ferric chloride and ferric sulphate. At various timepoints, ranging from  $t=0\text{h}$  to  $t=24\text{h}$ , the amount of  $^{55}\text{Fe}$  remaining in the medium has been evaluated by LSC. The composition of the LSC sample was based on the calibration curve as depicted in Figure C-1 of Appendix C. This yielded the composition shown in Table 8.

Compound	Amount (mL)
Ultima Gold Scintillation Cocktail	19.5 mL
Sample	0.5 mL

**Table 8.** Composition of the LSC samples.

The results of these measurements are depicted in Figures 14 and 15. Since the  $\text{OD}_{600}$ -values at  $t=24\text{h}$  are considered as being unreliable due to the early death of the organism, these have been left out of the results that will be discussed in the following sections.

##### 4.3.1. The uptake of supplemented $^{55}\text{Fe}$

To investigate the uptake of  $^{55}\text{Fe}$  by *E.coli*, the amount of  $^{55}\text{Fe}$  present in the LB-medium has been examined for various time points. Determination of the amount of  $^{55}\text{Fe}$  present in the medium is

indicative of the amount of  $^{55}\text{Fe}$  that is absorbed by *E.coli*, and therefore not present in the medium anymore.

In Figure 14, the relative amounts of  $^{55}\text{Fe}$  remaining in the LB-medium are depicted for 3 and 30  $\mu\text{M}$  iron supplementation with ferric chloride. Regarding iron supplementation of 3  $\mu\text{M}$  ferric chloride, an overall decrease of remaining iron in the medium is observed until  $t=3.5\text{h}$ . Between  $t=3.5\text{h}$  and  $t=4.5\text{h}$ , a small increase is observed, which is followed by a decrease. When considering 30  $\mu\text{M}$  iron supplementation, the overall amount of iron in the medium remains higher in comparison to 3  $\mu\text{M}$  iron supplementation. However, the differences between the supplementation of the two concentrations are not significant.

Since no significant differences can be observed between 3 and 30  $\mu\text{M}$  ferric chloride supplementation, this could be indicative that the main limiting factor of the growth of *E.coli* would not be the amount of iron present in the medium. This would be in correspondence with the findings from the growth experiments, as discussed in the previous section.

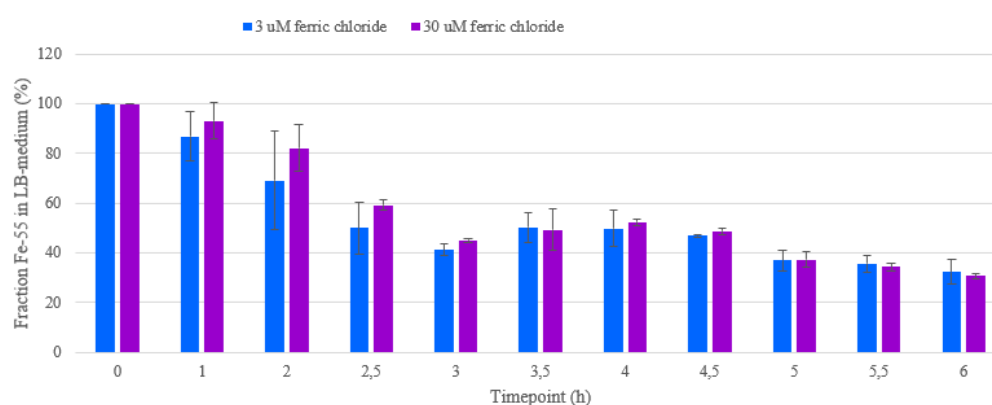


**Figure 14.** The relative amounts of  $^{55}\text{Fe}$  present in the medium are depicted for iron supplementation of 3 and 30  $\mu\text{M}$  of ferric chloride.

In Figure 15, the relative amounts of  $^{55}\text{Fe}$  remaining in the LB-medium are depicted for 3 and 30  $\mu\text{M}$  iron supplementation with ferric sulphate. For 3  $\mu\text{M}$  iron supplementation, a steady decrease in the amount of iron in the medium is observed until  $t=3.5\text{h}$ . From  $t=3.5$  an increase is observed in the amounts of  $^{55}\text{Fe}$  present in the medium. This increase is also observed for 30  $\mu\text{M}$  iron supplementation. Since the results do not reflect significant differences between either 3 or 30  $\mu\text{M}$  iron supplementation, this could again support that iron concentrations can not be considered as being the main limiting factor of the growth of *E.coli*.

In comparison to the results depicted in Figure 14, overall higher relative amounts are observed for supplementation with either 3 or 30  $\mu\text{M}$  ferric sulphate. This would be in accordance with the results obtained from the growth experiments, where overall lower values of  $\mu_{\text{max}}$  are reported for 30  $\mu\text{M}$  iron supplementation. Since no XRD-analysis has been done of the synthesised compound, it should be taken into account that either the expected compound was not synthesised.

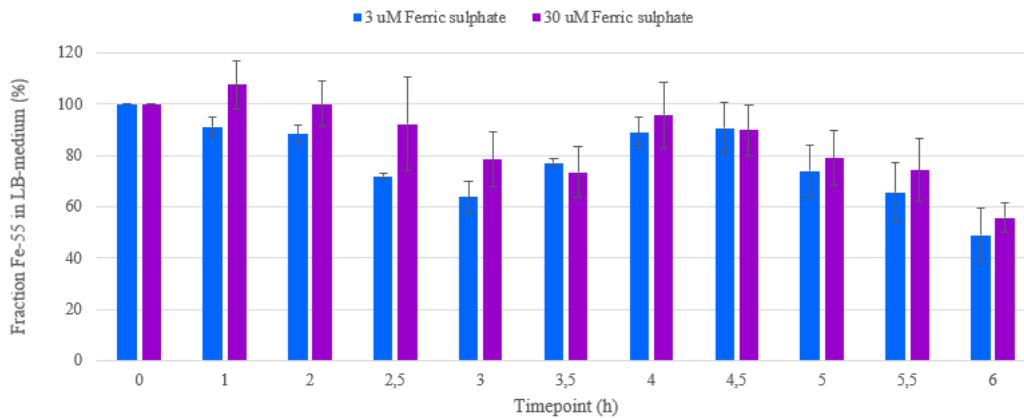


**Figure 15.** The relative amounts of  $^{55}\text{Fe}$  present in the medium are depicted for iron supplementation of 3 and 30  $\mu\text{M}$  of ferric sulphate.

#### 4.4. Further implications

*E.coli* has the capability to utilize both ferrous and ferric iron as a nutrient. Non-radioactive iron supplementation has shown an increase in the  $\mu_{\text{max}}$  for both ferrous and ferric sulphate. However, this increase is not observed when radioactive ferric chloride and ferric sulphate were supplemented. Research has shown that despite the capability of *E.coli* to utilize ferric iron as a nutrient through the formation of siderophores, the uptake of ferrous iron by *E.coli* seems more important than the transport of ferric iron (Kammler et al., 1993). This could explain the lowered value of the estimated  $\mu_{\text{max}}$ , and could account for lower uptake of ferric iron during the radionuclide supplementation experiments.

Since ID and IDA are treated with the supplementation of ferrous iron salts, *E.coli* will be provided with better growing conditions, and its virulence will be increased. Low concentrations of iron being supplemented already contribute to an enhanced environment for *E.coli* (Appenzeller et al., 2005; Hartmann & Braun, 1981; Ratledge & Winder, 1964). Therefore, in the treatment of ID and IDA, there should be aimed for concentrations as low as possible; aiming to still replenish iron stores, while minimizing the amount of unabsorbed iron that will be available for *E.coli*.

## 5. Conclusions and Recommendations

### 5.1. Conclusions

In this study, the successful synthesis of ferric sulphate and ferrous fumarate has been achieved.

However, the synthesis of ferrous sulphate was not successful. Therefore, it was impossible to perform growth experiments with supplementation of both radiolabelled ferrous sulphate and ferrous fumarate.

The growth experiments that have been conducted, indicate that the iron concentration could possibly not be the limiting factor of the growth of *E.coli*. Iron supplementation in the experiments where 50 mL Falcon tubes were used, resulted in an increase of the specific growth rate of a minimum of 26%. This indicates that the LB-medium was iron deficient. However, during the experiments where 250 mL round-bottom flasks were used, the estimated values of the specific growth rate were only slightly higher than those of the blanco measurements. In addition, 30  $\mu\text{M}$  supplementation of ferric sulphate even led to a decrease in the value of  $\mu_{\text{max}}$  in comparison to 3  $\mu\text{M}$  supplementation. This seems conflicting when it is taken into account that the iron concentration of the LB-medium used during these experiments is zero, whereas the LB-medium with Bacto™ Tryptone does contain small traces of iron. Therefore, no unambiguous conclusions can be drawn regarding the limiting factor of bacterial growth of *E.coli*.

The results obtained from the LSC measurements support the indication that iron concentrations may not be considered as the limiting factor of the growth of *E.coli* since no significant differences were observed between 3 and 30  $\mu\text{M}$  iron supplementation.

### 5.2. Recommendations

In order to investigate differences between the uptake of divalent and trivalent iron supplementation, it is recommended to perform growth experiments as described in section 3.2.4.3.3., with radioactive ferrous sulphate. One way these experiments could be conducted, would be by the irradiation of ferrous sulphate, after which it could be supplemented at concentrations of 3 and 30  $\mu\text{M}$ . In addition, irradiated ferrous sulphate could be used for the synthesis of ferrous fumarate.

Once the synthesis of ferrous fumarate using irradiated ferrous sulphate has been conducted successfully, it can be used as iron supplementation in growth experiments as well. However, ferrous fumarate is slightly soluble in water. Higher solubility is achieved in pH ranges of dilute acid. Therefore, difficulties could be encountered when using unmodified LB-medium with a pH equal to 7, as has been used during this study. However, as listed in Table 2, the pH of the duodenum lies between 1.5 – 4.5. Hence, it is recommended to perform further research into growth experiments at pH levels which are more representative of the environment of the gastrointestinal tract; lower pH levels could be investigated, simulating the environment in the duodenum. This could provide opportunities as well to investigate the influence of ferrous fumarate supplementation, since it is frequently used as a supplement to battle IDA. Furthermore, investigating a more diverse range of iron compounds as a supplement would be recommended.

Further research is recommended with respect to the growth conditions of *E.coli*. Performing experiments with different sizes of growth vessels is recommended, as significant differences have been observed between the values of the estimated growth parameters of 50 mL Falcon tubes and 250 mL round-bottom flasks. However, to be able to derive well-grounded conclusions, the same batch of LB-medium should be used throughout the experiments; therefore only changing one variable. Since it has been reported that the composition of LB-medium varies, there is more difficulty in reproducing experiments, and it is recommended to produce large batches of medium (Sezonov et al., 2007). Therefore, it is recommended to perform research into other growth media, and investigate whether reproducible results will be obtained. Additionally, it is recommended to investigate whether the LB-medium contains other nutrients, which nutrients, and at which concentration they are present. These nutrients could possibly compensate for the lack of iron present in the medium. To conduct this research, further analysis with ICP-OES is recommended.

The reported SD-values of the LSC analysis were relatively high, it is recommended to execute the growth experiments and LSC analysis more often. Despite that it is shown that ferric iron supplementation has a positive effect on the growth rate of *E.coli*, synthesised ferric sulphate did not seem to have a significantly positive effect on the growth of *E.coli* (Hartmann & Braun, 1981), Therefore, it is recommended to investigate 1) whether the synthesised compound was indeed ferric sulphate, 2) whether the amount of impurities is reduced as much as possible, and 3) how the growth of *E.coli* and the uptake of iron is affected by supplementation of radiolabelled ferrous compounds. Otherwise, other rinsing agents should be investigated for their potential of removing impurities.

## Bibliography

- Abbaspour, N., Hurrell, R., & Kelishadi, R. (2014). Review on iron and its importance for human health. *Journal of Research in Medical Sciences, 19*, 164–174.
- Anaemia*. (n.d.). Retrieved September 13, 2021, from [https://www.who.int/health-topics/anaemia#tab=tab\\_1](https://www.who.int/health-topics/anaemia#tab=tab_1)
- Appenzeller, B. M. R., Yañez, C., Jorand, F., & Block, J.-C. (2005). Advantage Provided by Iron for *Escherichia coli* Growth and Cultivability in Drinking Water. *Applied and Environmental Microbiology, 71*(9), 5621–5623. <https://doi.org/10.1128/AEM.71.9.5621-5623.2005>
- Bashiri, A., Burstein, E., Sheiner, E., & Mazor, M. (2003). Anaemia during pregnancy and treatment with intravenous iron: review of the literature. *European Journal of Obstetrics & Gynecology and Reproductive Biology, 110*(1), 2–7. [https://doi.org/10.1016/S0301-2115\(03\)00113-1](https://doi.org/10.1016/S0301-2115(03)00113-1)
- Berber, I., Diri, H., Erkurt, M. A., Aydogdu, I., Kaya, E., & Kuku, I. (2014). Clinical Study Evaluation of Ferric and Ferrous Iron Therapies in Women with Iron Deficiency Anaemia. *Advances in Hematology, 1*–6. <https://doi.org/10.1155/2014/297057>
- Bloor, S. R., Schutte, R., & Hobson, A. R. (2021a). Oral Iron Supplementation—Gastrointestinal Side Effects and the Impact on the Gut Microbiota. *Microbiology Research, 12*(2), 491–502. <https://doi.org/10.3390/MICROBIOLRES12020033>
- Bloor, S. R., Schutte, R., & Hobson, A. R. (2021b). Oral Iron Supplementation—Gastrointestinal Side Effects and the Impact on the Gut Microbiota. *Microbiology Research, 12*, 491–502. <https://doi.org/10.3390/MICROBIOLRES12020033>
- Brannon, P., & Taylor, C. (2017). Iron Supplementation during Pregnancy and Infancy: Uncertainties and Implications for Research and Policy. *Nutrients, 9*(12), 17. <https://doi.org/10.3390/nu9121327>
- Braun, V. (2003). IRON UPTAKE BY ESCHERICHIA COLI. *Frontiers in Bioscience, 8*, 1409–1421.
- Bunaciu, A. A., Udriștioiu, E. G., & Aboul-Enein, H. Y. (2015). X-Ray Diffraction: Instrumentation and Applications. *Critical Reviews in Analytical Chemistry, 45*(4), 289–299. <https://doi.org/10.1080/10408347.2014.949616>
- Busti, F., Marchi, G., & Girelli, D. (2019). Iron replacement in inflammatory bowel diseases: an evolving scenario. *Internal and Emergency Medicine 2019, 14*(3), 349–351. <https://doi.org/10.1007/S11739-019-02043-1>
- Camaschella, C. (2015). Iron-Deficiency Anemia. *New England Journal of Medicine, 372*(19), 1832–1843. <https://doi.org/10.1056/NEJMRA1401038>
- Chu, B. C., Garcia-Herrero, A., Johanson, T. H., Krewulak, K. D., Lau, C. K., Peacock, R. S., Slavinskaya, Z., & Vogel, H. J. (2010). Siderophore uptake in bacteria and the battle for iron with the host; a bird's eye view. *BioMetals, 23*(4), 601–611. <https://doi.org/10.1007/S10534-010-9361-X>
- Dalgaard, P., Ross, T., Kamperman, L., Neumeyer, K., & McMeekin, T. A. (1994). Estimation of bacterial growth rates from turbidimetric and viable count data. *International Journal of Food Microbiology, 23*(3–4), 391–404. [https://doi.org/10.1016/0168-1605\(94\)90165-1](https://doi.org/10.1016/0168-1605(94)90165-1)
- Demir, M., & Kaleli, I. (2004). Production by *Escherichia coli* isolates of siderophore and other virulence factors and their pathogenic role in a cutaneous infection model. *Clinical Microbiology and Infection, 10*(11), 1011–1014. <https://doi.org/10.1111/J.1469-0691.2004.01001.X>

- Dev, S., & Babitt, J. L. (2017). Overview of iron metabolism in health and disease. *Hemodialysis International*, 21, S6–S20. <https://doi.org/10.1111/hdi.12542>
- Elmagirbi, A., Sulistyarti, H., & Atikah, A. (2012). Study of ascorbic acid as iron (III) reducing agent for spectrophotometric iron speciation. *The Journal of Pure and Applied Chemistry Research*, 1(1), 11–17. <https://jpacr.ub.ac.id/index.php/jpacr/article/view/101>
- Estadella, J., Villamarín, L., Feliu, A., Perelló, J., & Calaf, J. (2018). Characterization of the population with severe iron deficiency anemia at risk of requiring intravenous iron supplementation. *European Journal of Obstetrics & Gynecology and Reproductive Biology*, 224, 41–44. <https://doi.org/10.1016/J.EJOGRB.2018.03.005>
- Finlayson-Trick, E. C., Fischer, J. A., Goldfarb, D. M., & Karakochuk, C. D. (2020). The effects of iron supplementation and fortification on the gut microbiota: a review. *Gastrointestinal Disorders*, 2(4), 327–340. <https://doi.org/10.3390/gidisord2040030>
- Gibson, J. A. B., & Lally, A. E. (1971). Liquid Scintillation Counting as an Analytical Tool. A review. *The Analyst*, 681–688.
- Gómez-Ramírez, S., Brilli, E., Tarantino, G., & Muñoz, M. (2018). Sucrosomial® Iron: A New Generation Iron for Improving Oral Supplementation. *Pharmaceuticals*, 1–23. <https://doi.org/10.3390/ph11040097>
- Gupta, P., Lakes, A., & Dziubla, T. (2016). A Free Radical Primer. *Oxidative Stress and Biomaterials*, 1–33. <https://doi.org/10.1016/B978-0-12-803269-5.00001-2>
- Hartmann, A., & Braun, V. (1981). Iron Uptake and Iron Limited Growth of Escherichia coli K-12. *Arch Microbiol*, 130, 353–356.
- Helmyati, S., Rahayu, E. S., Kandarina, B. J. I., & Juffrie, M. (2018). No Difference Between Iron Supplementation Only and Iron Supplementation with Synbiotic Fermented Milk on Iron Status, Growth, and Gut Microbiota Profile in Elementary School Children with Iron Deficiency. *Current Nutrition & Food Science*, 16(2), 220–227. <https://doi.org/10.2174/1573401314666181017110706>
- Hurrell, R., & Egli, I. (2010). Iron bioavailability and dietary reference values. *The American Journal of Clinical Nutrition*, 91(5), 1461S–1467S. <https://doi.org/10.3945/AJCN.2010.28674F>
- Jaeggi, T., Kortman, G. A. M., Moretti, D., Chassard, C., Holding, P., Dostal, A., Boekhorst, J., Timmerman, H. M., Swinkels, D. W., Tjalsma, H., Njenga, J., Mwangi, A., Kvalsvig, J., Lacroix, C., & Zimmermann, M. B. (2015). Iron fortification adversely affects the gut microbiome, increases pathogen abundance and induces intestinal inflammation in Kenyan infants. *Gut*, 64(5), 731–742. <https://doi.org/10.1136/gutjnl-2014-307720>
- Jahn, M. R., Andreasen, H. B., Fütterer, S., Nawroth, T., Schünemann, V., Kolb, U., & Langguth, P. (2011). A comparative study of the physicochemical properties of iron isomaltoside 1000 (Monofer®), a new intravenous iron preparation and its clinical implications. *European Journal of Pharmaceutics and Biopharmaceutics*, 78(3), 480–491. [https://www.sciencedirect.com/science/article/pii/S0939641111001172?casa\\_token=DsdZritCtX8AAAAA:qGNPqCagKD1LJbkCE3kUBRCYqRjP4AjryFI39O13caPNmqQTwxca8JXG0u4bbQICWb0h3rldOQRt](https://www.sciencedirect.com/science/article/pii/S0939641111001172?casa_token=DsdZritCtX8AAAAA:qGNPqCagKD1LJbkCE3kUBRCYqRjP4AjryFI39O13caPNmqQTwxca8JXG0u4bbQICWb0h3rldOQRt)
- Jia, H. X., Han, J. H., Li, H. Z., Liang, D., Deng, T. T., & Chang, S. Y. (2016). Mineral Intake in Urban Pregnant Women from Base Diet, Fortified Foods, and Food Supplements: Focus on Calcium, Iron, and Zinc. *Biomedical and Environmental Sciences*, 29(12), 898–901.

<https://www.besjournal.com/fileSWYXYHJKX/journal/article/swyxyhjkx/2016/12/PDF/20161207.pdf>

- Kammler, M., Schon, C., & Hantke, K. (1993). Characterization of the Ferrous Iron Uptake System of *Escherichia coli*. *JOURNAL OF BACTERIOLOGY*, *175*(19), 6212–6219.  
<https://journals.asm.org/journal/jb>
- Kansara, K., Patel, P., Shukla, R. K., Pandya, A., Shanker, R., Kumar, A., & Dhawan, A. (2018). Synthesis of biocompatible iron oxide nanoparticles as a drug delivery vehicle. *International Journal of Nanomedicine*, *13*, 79–82. <https://doi.org/10.2147/IJN.S124708>
- Kapor, A. J., Nikolic, L. B., Nikolic, V. D., Stankovic, M. Z., Cacic, M. D., Ilic, D. P., & Ristic, I. S. (2012). The synthesis and characterization of iron (II) fumarate with cyclodextrins. *Advanced Technologies*, *1*(1), 7–15.
- Kehrer, J. P. (2000). The Haber–Weiss reaction and mechanisms of toxicity. *Toxicology*, *149*(1), 43–50.  
[https://www.sciencedirect.com/science/article/pii/S0300483X00002316?casa\\_token=IOhA4Q3m80cAAAAA:uTdQWHkc1ir1DzqXVY6H8WwDgpEHPbGnO86bwezbsc-t3mJvoehmzymz1P3Ks7wFG-C9ojPU](https://www.sciencedirect.com/science/article/pii/S0300483X00002316?casa_token=IOhA4Q3m80cAAAAA:uTdQWHkc1ir1DzqXVY6H8WwDgpEHPbGnO86bwezbsc-t3mJvoehmzymz1P3Ks7wFG-C9ojPU)
- Kortman, G. A., Raffatellu, M., Swinkels, D. W., & Tjalsma, H. (2014). Nutritional iron turned inside out: intestinal stress from a gut microbial perspective. *FEMS Microbiology Reviews*, *38*, 1202–1234. <https://academic.oup.com/femsre/article-abstract/38/6/1202/552682>
- Krumova, K., & Cosa, G. (2016). *Overview of Reactive Oxygen Species*.  
<https://doi.org/10.1039/9781782622208-00001>
- Lessard, J. C. (2013). Chapter Eleven - Growth Media for *E. coli*. *Methods in Enzymology*, *533*, 181–189. <https://doi.org/10.1016/B978-0-12-420067-8.00011-8>
- Livechart - Table of Nuclides - Nuclear structure and decay data*. (n.d.). Retrieved June 27, 2022, from <https://www-nds.iaea.org/relnsd/vcharthtml/VChartHTML.html>
- Lugtenberg, B., & van Alphen, L. (1983). Molecular architecture and functioning of the outer membrane of *Escherichia coli* and other gram-negative bacteria. *Biochimica et Biophysica Acta (BBA)-Reviews on Biomembranes*, *737*(1), 51–115. [https://doi.org/10.1016/0304-4157\(83\)90014-X](https://doi.org/10.1016/0304-4157(83)90014-X)
- Martin, P., Tronnet, S., Garcie, C., & Oswald, E. (2017). Interplay between siderophores and colibactin genotoxin in *Escherichia coli*. *IUBMB Life*, *69*(6), 435–441.  
<https://doi.org/10.1002/IUB.1612>
- Martínez-Navarrete, N., Camacho, M. M., Martínez-Lahuerta, J., Martínez-Monzó, J., & Fito, P. (2002). Iron deficiency and iron fortified foods - A review. *Food Research International*, *35*(2–3), 225–231. [https://doi.org/10.1016/S0963-9969\(01\)00189-2](https://doi.org/10.1016/S0963-9969(01)00189-2)
- McKellar, R. C., Pérez-Rodríguez, F., Harris, L. J., Moyne, A.-L., Blais, B., Topp, E., Bezanson, G., Bach, S., & Delaquis, P. (2014). Evaluation of different approaches for modeling *Escherichia coli* O157:H7 survival on field lettuce. *International Journal of Food Microbiology*, *184*, 74–85.  
<https://doi.org/10.1016/j.ijfoodmicro.2014.04.026>
- Meneghini, R. (1997). Iron homeostasis, oxidative stress, and DNA damage. *Free Radical Biology & Medicine*, *23*(5), 783–792.

- Miethke, M., & Marahiel, M. A. (2007). Siderophore-Based Iron Acquisition and Pathogen Control. *Microbiology and Molecular Biology Reviews*, 413–451. <https://doi.org/10.1128/MMBR.00012-07>
- Nagpal, J., & Choudhury, P. (2004). Iron Formulations in Pediatric Practice. *Indian Pediatrics*, 41(8), 807–815.
- Neiser, S., Rentsch, D., Kappler, A., Weidler, P. G., Göttlicher, J., & Burckhardt, S. (2015). Physico-chemical properties of the new generation IV iron preparations ferumoxytol, iron isomaltoside 1000 and ferric carboxymaltose. *Biometals*, 28(4), 615–635. <https://doi.org/10.1007/s10534-015-9845-9>
- Noor, R., Islam, Z., Munshi, S. K., & Rahman, F. (2014). Influence of Temperature on Escherichia coli Growth in Different Culture Media. *Journal of Pure and Applied Microbiology*, 899–904. <https://www.researchgate.net/publication/233761514>
- Olesik, J. W. (1991). Elemental analysis using ICP-OES and ICP-MS. *Analytical Chemistry*, 63(1), 12A-21A. <https://pubs.acs.org/sharingguidelines>
- Pagani, A., Nai, A., Silvestri, L., & Camaschella, C. (2019). Hepcidin and Anemia: A Tight Relationship. *Frontiers in Physiology | Www.Frontiersin.Org*, 10, 1–7. <https://doi.org/10.3389/fphys.2019.01294>
- Paganini, D., & Zimmerman, M. B. (2017). The effects of iron fortification and supplementation on the gut microbiome and diarrhea in infants and children: a review. *The American Journal of Clinical Nutrition*, 106, 1688S-1693S. <https://doi.org/10.3945/ajcn>
- Papanikolaou, G., & Pantopoulos, K. (2005). Iron metabolism and toxicity. *Toxicology and Applied Pharmacology*, 202(2), 199–211. <https://doi.org/10.1016/J.TAAP.2004.06.021>
- Patil, S. S., Khanwelkar, C. C., Patil, S. K., Thorat, V. M., Jadhav, S. A., & Sontakke, A. v. (2013). Comparison of efficacy, tolerability, and cost of newer with conventional oral iron preparation. *Al Ameen Journal of Medical Sciences*, 6(1), 29–33.
- Pérez-Conesa, D., López, G., Abellán, P., & Ros, G. (2006). Bioavailability of calcium, magnesium and phosphorus in rats fed probiotic, prebiotic and synbiotic powder follow-up infant formulas and their effect on physiological and nutritional parameters. *Journal of the Science of Food and Agriculture*, 86(14), 2327–2336. <https://doi.org/10.1002/JSFA.2618>
- PerkinElmer. (n.d.-a). *Liquid Scintillation Cocktails*.
- PerkinElmer. (n.d.-b). *Quench, Counting Efficiency, and Quench Correction*. Retrieved July 21, 2022, from <https://www.perkinelmer.com/nl/lab-products-and-services/application-support-knowledgebase/radiometric/quench.html#Quenchcountingefficiencyandquenchcorrection-tSIE>
- Podgórna, K., & Szczepanowicz, K. (2016). Synthesis of polyelectrolyte nanocapsules with iron oxide (Fe<sub>3</sub>O<sub>4</sub>) nanoparticles for magnetic targeting. *Colloids and Surfaces A: Physicochemical and Engineering Aspects*, 505, 132–137. <https://doi.org/10.1016/J.COLSURFA.2016.02.017>
- Pommé, S., Stroh, H., & van Ammel, R. (2019). The <sup>55</sup>Fe half-life measured with a pressurised proportional counter. *Applied Radiation and Isotopes*, 148, 27–34. <https://doi.org/10.1016/J.APRADISO.2019.01.008>
- Qi, X., Zhang, Y., Guo, H., Hai, Y., Luo, Y., & Yue, T. (2020). Mechanism and intervention measures of iron side effects on the intestine. *Critical Reviews in Food Science and Nutrition*, 60(12), 2113–2125. <https://doi.org/10.1080/10408398.2019.1630599>

- Ratledge, C., & Winder, F. G. (1964). Effect Of Iron And Zinc On Growth Patterns Of Escherichia Coli In An Iron-Deficient Medium. *JOURNAL OF BACTERIOLOGY*, 87(4), 823–827. <https://journals.asm.org/journal/jb>
- Rusu, I., Suharoschi, R., Vodnar, D., Pop, C. R., Socaci, S. A., Vulturar, R., & Pop, O. L. (2020). Iron supplementation influence on the gut microbiota and probiotic intake effect in iron deficiency— A literature-based review. *Nutrients*, 12, 1–16. <https://doi.org/10.3390/nu12071993>
- Santiago, P. (2012). Ferrous versus ferric oral iron formulations for the treatment of iron deficiency: A clinical overview. *The Scientific World Journal*. <https://doi.org/10.1100/2012/846824>
- Schaefer, B., Meindl, E., Wagner, S., Tilg, H., & Zoller, H. (2020). Intravenous iron supplementation therapy. *Molecular Aspects of Medicine*, 75, 1–7. <https://doi.org/10.1016/J.MAM.2020.100862>
- Sezonov, G., Joseleau-Petit, D., & D'Ari, R. (2007). Escherichia coli Physiology in Luria-Bertani Broth. *Journal of Bacteriology*, 189, 8746–8749. <https://doi.org/10.1128/JB.01368-07>
- Sneddon, J., & Vincent, M. D. (2008). ICP-OES and ICP-MS for the Determination of Metals: Application to Oysters. *Analytical Letters*, 41(8), 1291–1303. <https://doi.org/10.1080/00032710802013991>
- Souza, A. D., Pina, P. S., Leão, V. A., Silva, C. A., & Siqueira, P. F. (2007). The leaching kinetics of a zinc sulphide concentrate in acid ferric sulphate. *Hydrometallurgy*, 89(1–2), 72–81. <https://doi.org/10.1016/J.HYDROMET.2007.05.008>
- Stanjek, H., & Häusler, W. (2004). Basics of X-ray Diffraction. *Hyperfine Interactions*, 154(1), 107–119.
- Stelle, I., Kalea, A. Z., & Pereira, D. I. A. (2018). Iron deficiency anaemia: experiences and challenges. *Proceedings of the Nutrition Society*, 78, 19–26. <https://doi.org/10.1017/S0029665118000460>
- Stoffel, N. U., von Siebenthal, H. K., Moretti, D., & Zimmermann, M. B. (2020). Oral iron supplementation in iron-deficient women: How much and how often? *Molecular Aspects of Medicine*, 75, 1–9. <https://doi.org/10.1016/J.MAM.2020.100865>
- Stoltzfus, R. J. (2003). Iron deficiency : Global prevalence and consequences. *Food and Nutrition Bulletin*, 24(4), S99–S103.
- Stoltzfus, R. J., & Dreyfuss, M. L. (1998). *Guidelines for the use of iron supplements to prevent and treat iron deficiency anemia* (Vol. 2). Ilsi Press. [http://www.health-mall.in/files\\_hl/guidelines\\_iron\\_supplementation.pdf](http://www.health-mall.in/files_hl/guidelines_iron_supplementation.pdf)
- Straub, K. L., Benz, M., & Schink, B. (2000). Iron metabolism in anoxic environments at near neutral pH. *FEMS Microbiology Ecology*, 34(3), 181–186. <https://doi.org/10.1111/j.1574-6941.2001.tb00768.x>
- Tachibana, S., Chiou, T. Y., & Konishi, M. (2021). Machine learning modeling of the effects of media formulated with various yeast extracts on heterologous protein production in Escherichia coli. *MicrobiologyOpen*, 10, 1–14. <https://doi.org/10.1002/MBO3.1214>
- Tapiero, H., Gaté, L., & Tew, K. D. (2001). Iron: deficiencies and requirements. *Biomedicine & Pharmacotherapy*, 55(6), 324–332. [https://doi.org/10.1016/S0753-3322\(01\)00067-1](https://doi.org/10.1016/S0753-3322(01)00067-1)
- Tolkien, Z., Stecher, L., Mander, A. P., Pereira, D. I. A., & Powell, J. J. (2015). Ferrous Sulfate Supplementation Causes Significant Gastrointestinal Side-Effects in Adults: A Systematic Review and Meta-Analysis. *PloS One*, 1–20. <https://doi.org/10.1371/journal.pone.0117383>

- van Dijk, M. C. (2021). *A Game of Ions. The Importance of the Transition Metals Manganese and Iron to the Evasion of Nutritional Immunity by Staphylococcus aureus*. Technical University of Delft.
- Vogt, A.-C. S., Arsiwala, T., Mohsen, M., Vogel, M., Manolova, V., & Bachmann, M. F. (2021). Molecular Sciences On Iron Metabolism and Its Regulation. *International Journal*. <https://doi.org/10.3390/ijms22094591>
- Wandersman, C., & Delepelaire, P. (2004). Bacterial Iron Sources: From Siderophores to Hemophores. *Annu. Rev. Microbiol*, 58, 611–647. <https://doi.org/10.1146/annurev.micro.58.030603.123811>
- Yiannikourides, A., & Latunde-Dada, G. O. (2019). A Short Review of Iron Metabolism and Pathophysiology of Iron Disorders. *Medicines*, 6(85), 1–15. <https://doi.org/10.3390/MEDICINES6030085>
- Yilmaz, B., & Li, H. (2018). Gut Microbiota and Iron: The Crucial Actors in Health and Disease. *Pharmaceuticals*, 11(4), 20. <https://doi.org/10.3390/PH11040098>
- Zwietering, M. H., Jongenburger, I., Rombouts, F. M., & van het Riet, K. J. A. E. M. (1990). Modeling of the Bacterial Growth Curve PUM. *Applied and Environmental Microbiology*, 56(6), 1875–1881. <https://journals.asm.org/journal/aem>

## Appendix A – Growth curve experiments with non-radioactive iron supplementation

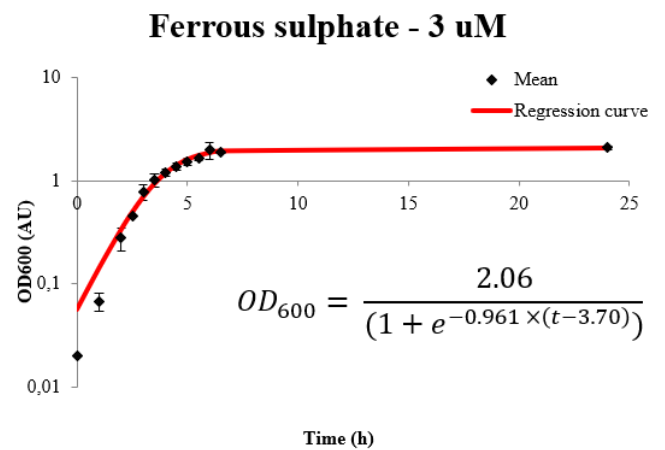
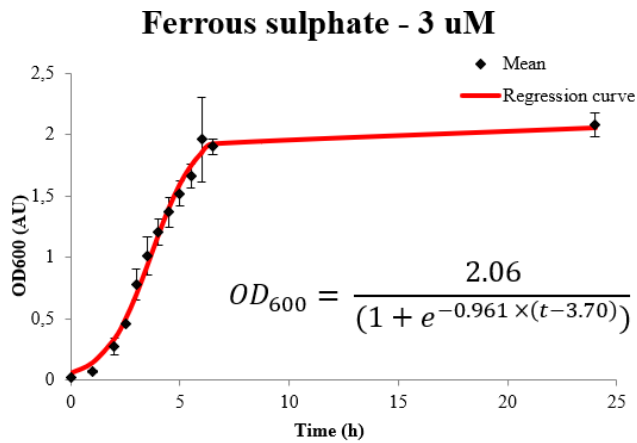


**Figure A-1.** Mean growth behaviour of *E.coli* on LB-medium containing Bacto™ Yeast Extract. 3  $\mu$ M ferrous sulphate was supplemented. Growth experiments were performed in 50 mL Falcon tubes.. The mean (left) and log-scale (right) growth curves were fitted by OLS.

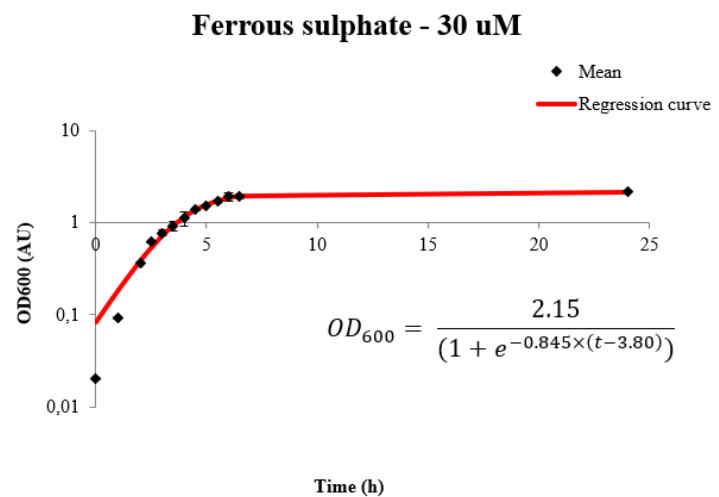
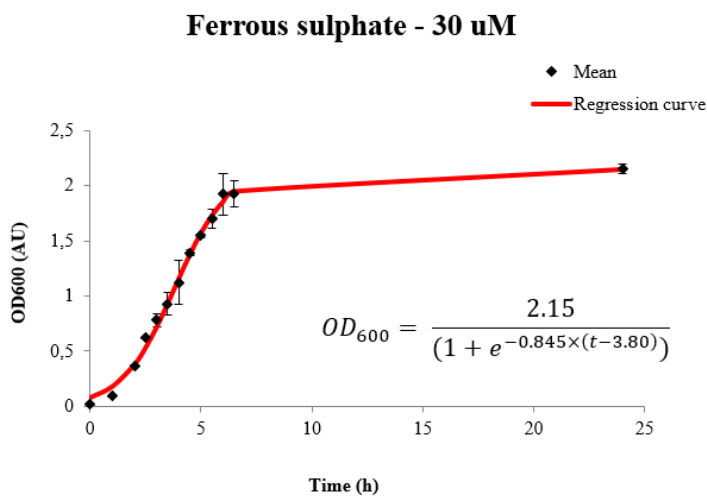
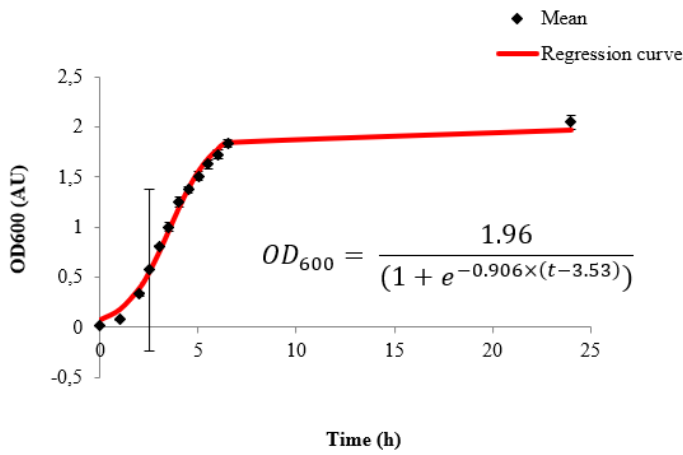


**Figure A-2.** Mean growth behaviour of *E.coli* on LB-medium containing Bacto™ Yeast Extract. 30  $\mu$ M ferrous sulphate was supplemented. Growth experiments were performed in 50 mL Falcon tubes.. The mean (left) and log-scale (right) growth curves were fitted by OLS.

### Ferric sulphate - 3 uM



### Ferric sulphate - 3 uM

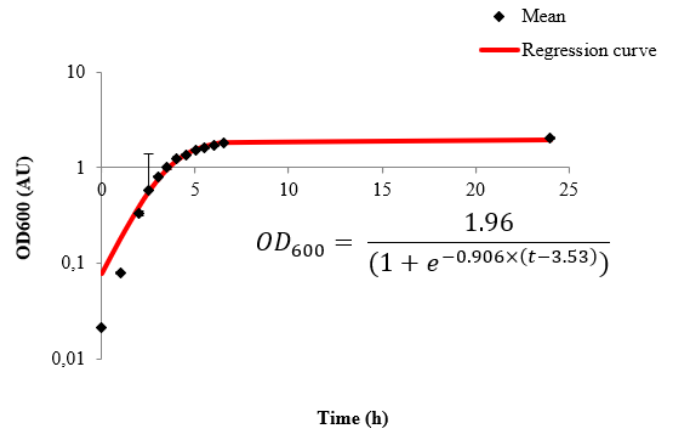
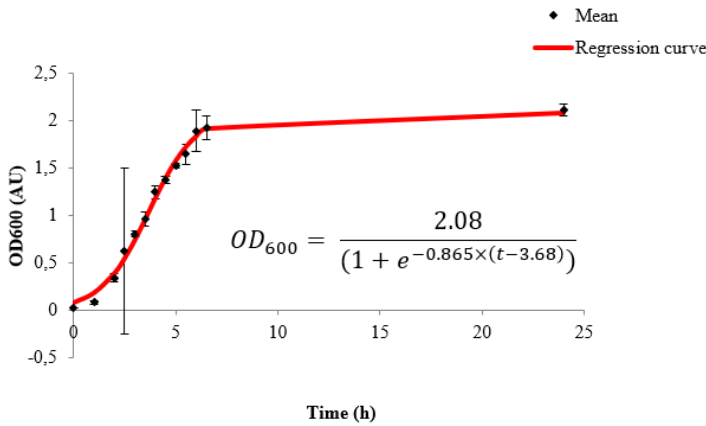


**Figure A-3.** Mean growth behaviour of *E. coli* on LB-medium containing Bacto™ Yeast Extract. 3 uM ferric sulphate was supplemented. Growth experiments were performed in 50 mL Falcon tubes.. The mean (left) and log-scale (right) growth curves were fitted by OLS.

### Ferric sulphate - 30 uM



### Ferric sulphate - 30 uM

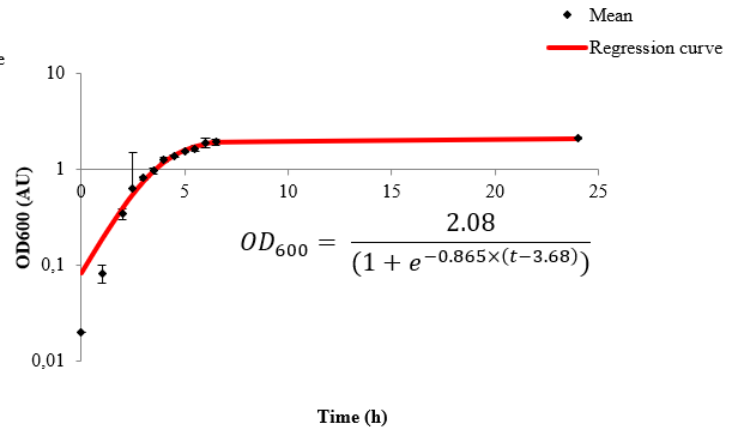


**Figure A-4.** Mean growth behaviour of *E. coli* on LB-medium containing Bacto™ Yeast Extract. 30 uM ferric sulphate was supplemented. Growth experiments were performed in 50 mL Falcon tubes.. The mean (left) and log-scale (right) growth curves were fitted by OLS.

## Appendix B – Growth curve experiments with radionuclide iron supplementation

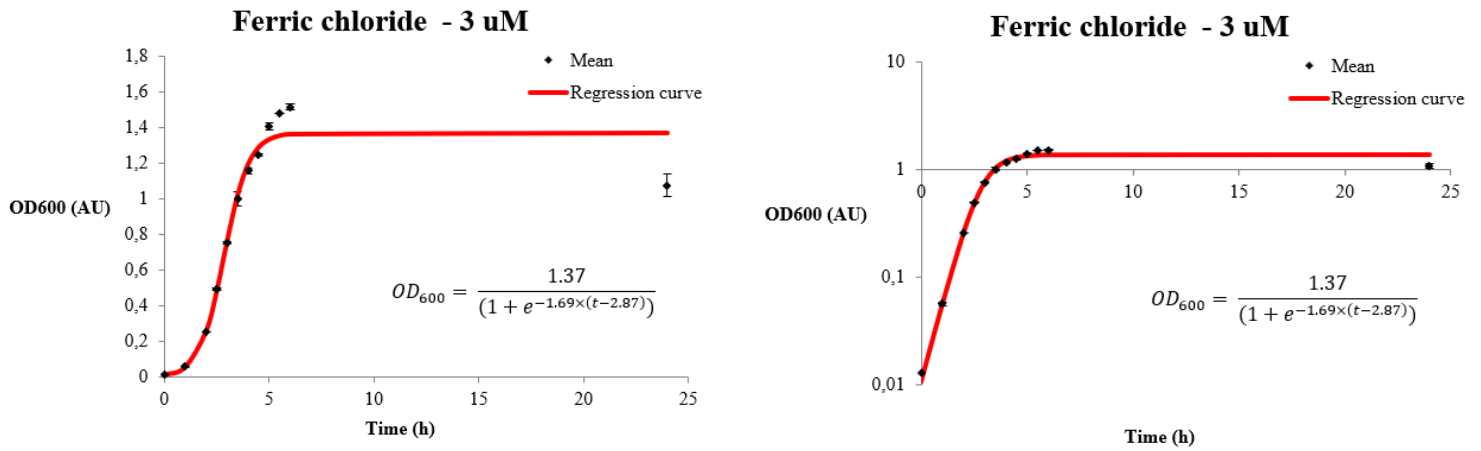


**Figure B-1.** Mean growth behaviour of *E. coli* on LB-medium containing Yeast Extract. 3 µM ferric chloride was supplemented. Growth experiments were performed in 250 mL round-bottom flasks. The mean (left) and log-scale (right) growth curves were fitted by OLS.

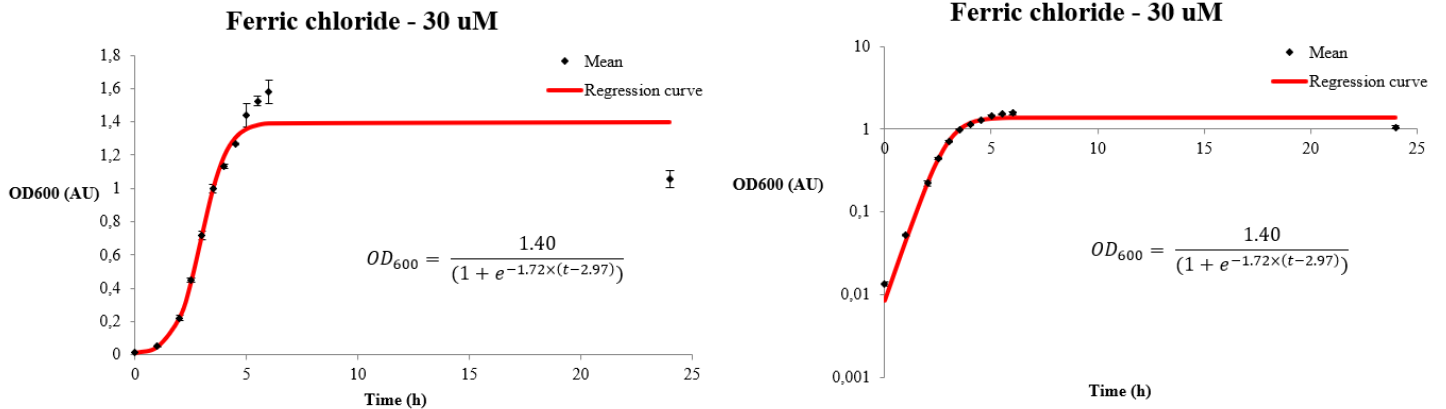


**Figure B-2.** Mean growth behaviour of *E. coli* on LB-medium containing Yeast Extract. 30 µM ferric chloride was supplemented. Growth experiments were performed in 250 mL round-bottom flasks. The mean (left) and log-scale (right) growth curves were fitted by OLS.

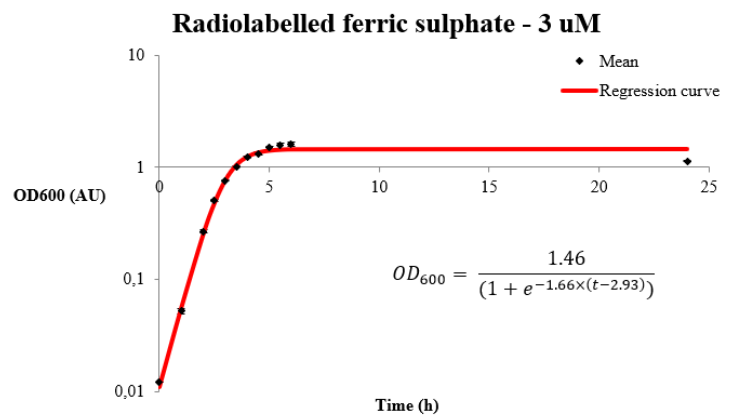
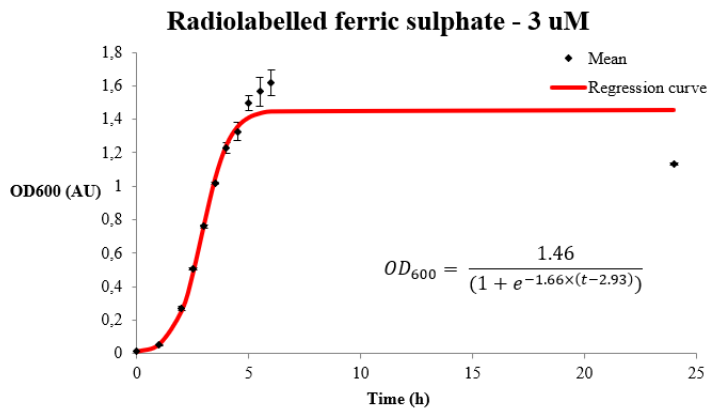


**Figure B-3.** Mean growth behaviour of *E.coli* on LB-medium containing Yeast Extract. 3  $\mu\text{M}$  ferric sulphate was supplemented. Growth experiments were performed in 250 mL round-bottom flasks. The mean (left) and log-scale (right) growth curves were fitted by OLS.

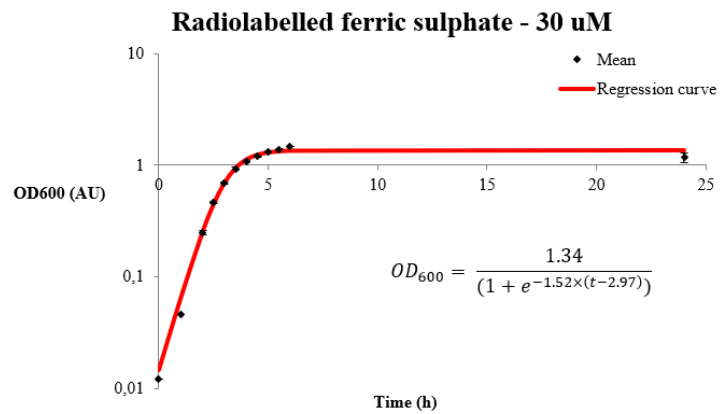
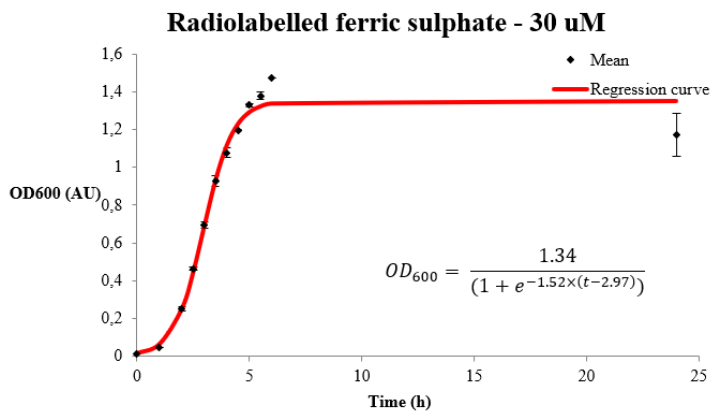


**Figure B-4.** Mean growth behaviour of *E.coli* on LB-medium containing Yeast Extract. 30  $\mu\text{M}$  ferric sulphate was supplemented. Growth experiments were performed in 250 mL round-bottom flasks. The mean (left) and log-scale (right) growth curves were fitted by OLS.

## Appendix C – Liquid Scintillation Counting – Construction of a quench correction curve

As described in section 2.6.2., LSC measurements are paired with various forms of quenching. The amount of quenching can be assessed by the value of tSIE; where no quenching is represented with a value of 1000.

To construct the quench correction curve, and determine the optimal amount of solution that should be added, varying amounts of LB-medium (0.1 mL – 1 mL) were added to the scintillation cocktail. However, when only 10 mL scintillation cocktail was used, a two-phase system was created. Therefore, using only 10 mL scintillation cocktail was deemed unsuitable, and further measurements to construct the quenching curve were done with amounts of LB-medium ranging from 19 mL to 20 mL. To each vial, 10  $\mu$ L of the  $^{55}\text{FeCl}_3$ -stock solution was added. The resulting quench curve is shown in Figure C.1. Based on the quench correction curve, for the remaining measurements, the composition for each counting vial was chosen, as depicted in Table 8.

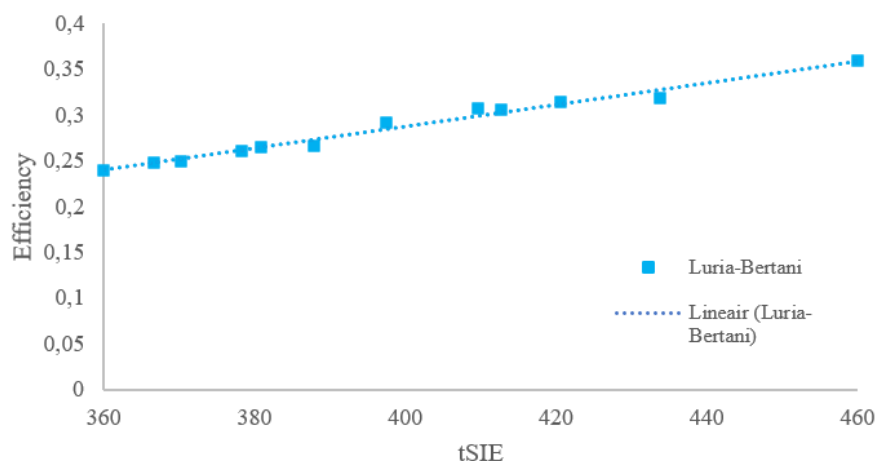


**Figure C-1.** The constructed quench correction curve. The quenching material was a solution of LB-medium. A linear fit is added by the automatic function of Excel, resulting in the function  $y = 0.0012x - 0.1876$ , and  $R^2 = 0.98$ .